A NON-EXTENSIVE STATISTICS APPROACH OF SEISMIC CODA WAVES.

Evidence In Earthquake Events of Greece And Italy

MS.c IN "GEO-ENVIRONMENTAL RESOURCES AND RISKS" THESIS WORK

20/12/2018

KOUTALONIS IOANNIS

The future belongs to those who possess different skills…
And combine them in creative ways….
Thanks to everyone who helped me be creative…..
Thanks to everyone who offered me the future….

Table of contents

Abstract

Investigation of dynamical features of Earthquake records is one of the important scientific and practical research challenges. In the addition there is a growing interest concerning an approach to study Earth Physics based on the science of complexity, focusing on the application of non extensive statistical mechanics, which is a generalization of Boltzmann-Gibbs statistical physics.

This seems to be a promising framework for studying complex systems as that of seismicity exhibiting phenomena such as, long-range interactions, and memory effects. In this work we use the framework of non-extensive statistical mechanics to explore the nature of seismic coda waves.

A system that follows Boltzmann-Gibbs statistical mechanics has to follow the well known Gaussian form. In the same manner a system that follows non-extensive statistical mechanics has to follow the q-Gaussian distribution. The main feature of q-Gaussian distribution is the parameter "q" which is often called the non additivity index.

In the present work we analyzed the fluctuations of seismic coda waves that follow the primary waves on an earthquake record. Following the non extensive statistical physics approach, the probability distribution functions of the increments of seismic coda are investigated.

We defined the function $X(t) = S(t + 1) - S(t)$, whereas $S(t)$ is the measured horizontal ground motion. We proceed by analyzing the normalized increments $X(t)$ constructing the probability density function $(PDF)p(x)$, normalized "x" to zero mean and unit variance, thus $x = \frac{x - \langle x \rangle}{\sigma_x}$ which express that the $PDF's$ associated with the normalized increments.

We also analyzed the frequency dependence of q, estimating the q value of the coda wave obtained after filtering the original coda waves applying spectrum of the seismic coda waves applying $2 \, \& \, 4 Hz$ windows and moving the central frequency in the frequency range of $2 - 16 HZ$.

Introduction

" Τά πάντα ῥεῖ "

…Said Heraclitus, which means that "Everything is in a constant movement". This Saying has proven to be true in all the scales composing the Cosmos, from the quantum microscale of uncertainty leading to quantum boiling to the planetary scale leading to the expanding universe. In the latter scale, and more specifically down to earth, this movement causes phenomena dangerous and deadly. The Composition and structure of the earth itself as we know it so far, forces the accumulation of stresses whose release causes earthquakes to occur.

Earthquake occurrence is an unavoidable phenomenon. The vast amounts of variables that compose their dynamics as well as their complexity make their secrets well hidden by scientists until now. In fact, earthquakes are omnipresent and little has been done until now for their prediction but a lot of existing research as well as the contribution of this work, place a promising framework for their utilization.

By taking advantage of the omnipresence of earthquakes and their produced signals, we will try to utilize the information they can give us about the earth's structure by using concepts of non-extensive statistical mechanics. More specifically, we will try to treat statistically the latter part of the seismogram that comes after the Primary and Secondary (P-WAVES and S-WAVES) which is called "Coda part of the seismogram or "Coda-waves".

1. Coda waves. Nature & Characteristics

Initially taken by the Latin word "Cauda"
which Means the extreme part/tail of anything,
a variant Of the word was taken to name
the tail of the surface Waves,
following the maximum displacement.

1.1. A FIRST INTERPRETATION

Since the first recording of Earthquakes, it was observed that the duration of the earthquake signal is much longer than the travel time of the ballistic waves [1]. Or similarly for local earthquakes, whose source durations are lower than $0.1\ sec$, the seismic energy is commonly recorded for hundreds of seconds after the direct S-wave.

In reality, in an earthquake waveform we observe the "P" and "S" waves followed by a decaying wave part ($Fig.\ 1$). The decaying part of the seismogram that extends later than the S-waves is called the Coda-wave or Coda-tail.

The term "decaying part" refers to the attenuation which indicates loss of energy in the seismic wave with travel distance and can be caused by conversion of elastic energy into heat (intrinsic attenuation) or by scattering from heterogeneities in the lithosphere [2,19]. The mechanism by which scattering constructs coda waves and contributes to their attenuation is still not completely understood due to its vast complexity.

The most prevalent reasoning about coda waves is that they are caused due to backscattering by heterogeneities distributed in the large region outside the zone of the direct wave path from the source to the station [2] but they are not regular plane waves coming directly from the epicenter. Small aperture arrays show that coda waves are coming by various ranrdom directions [3].
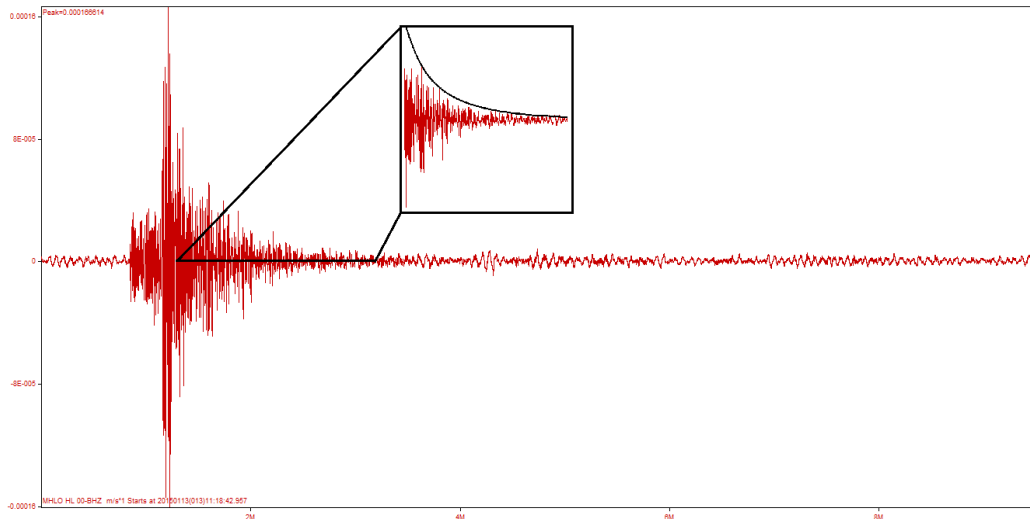
Figure 1: An actual seismic recording with the exponential tail or Coda-wave indicated.

More specifically, studying the existing literature we will try to dig deeper and understand more extensively about the nature of coda waves

1.2. NATURE OF CODA WAVES

Why can't coda waves just be waves with lower propagation speed? Such waves have been observed for oceanic paths and in land paths including water covered areas [32, 33].

If the coda waves observed in the close proximity stations were to travel at lower speeds that equals to speeds of $\sim 50 \, {}^m/_{sec}$ which is significantly low. Furthermore, in order for the same phenomenon to be true for further stations, we should assign velocities an order of magnitude higher, but these stations show similar spectral content.

Thus we assume that the nature of the waves that compose the coda does not differ from close-proximity to distant stations. This Fact holds in fact true for a wide spectrum of frequencies from $1 - 40 Hz$ [4].

Those difficulties disappear if we regard coda as backscattering waves coming from scatterers distributed over a large area surrounding the stations and epicenters. In order to have scattering though, we accept the fact that earth is inhomogeneous.

1.2.1. Inhomogeneous earth?

How do you deal with chaos?
You break it down in small pieces….non-chaotic
But in the end, it's still chaos…

Authors have realized that homogeneous earth properties are not sufficient to explain phenomena like Coda wave attenuation. That is the reason they try to insert elements in their models that make earth deviate from the ideal homogeneous case [7].

Examples like "homogeneous distribution of scattering mean free path" and "intrinsic absorption" [13] or "Stochastic random inhomogeneity" [14] have been widely implemented for studying the heterogeneities of the earth.

The complexity of the problem is even higher if we take into account the fact that the representation of small-scale variation of Earth's structure may be varied not only by the physical but also by the chemical environment as well. We are beginning to getting a grasp of the amount of complexity that is hidden within the Earth's crust

1.2.2. Seismic coda origins

Seismic coda can be produced by various sources according to the bibliography. One case is by scattering body waves by heterogeneities distributed through the lithosphere [2] or Surface waves scattered by lateral heterogeneities [7,8]. This is the most studied case and believed to be the most dominant.

Another assumption is from repercussions in horizontally layered structure under the receiver, also known as site response [11]. Or repercussions in layered structures between the source and the receiver [6, 11, 15]. Finally, other theories propose that Coda waves are produced by conversion of body waves into surface waves induced by topography at the free surface or at buried inter-phases at depth [9].

The main mechanism that we will deal in this work as mentioned is the first case. This mechanism proposes that primary waves spread radially outwards of the seismic source. Their nature depends on the local geology and the earth's structure along the wave path from source to station. Coda waves on the other hand, travel in the same manner but get scattered due to inhomogeneities in that waveguide and thus moving throughout multiple random directions [17].

The scale length of earth's inhomogeneous structure is coarser than the wavelengths of the seismic waves [13] and is of at least $10 - 8: 0.001 \ to \ 10,000 \ Km$ [10]. The inhomogeneity of earth's interior is known by studies using well-logs, short period seismograms and free oscillation data [11].

Those inhomogeneities affect the amplitude of the signal depending on their size. Their effect differ with their size [12]. Inhomogeneities Greater than the wavelength of the wavefront perturb $P, S-$wave travel times, where Inhomogeneities in the same sizes distort seismic wavefronts. Finally, if the size of the scatterers is smaller than the wavelength of the wavefront such as distributed cracks and velocity boundaries/gradients, they act as scatterers to the wave front. Due to those relations, the characteristics of earth's inhomogeneity define the characteristics of coda waves that travel through them. Those characteristics channel their complex nature to Coda waves.

There is a vast difference between the composition of early coda and the late coda. This happens because the longer the waves travel, the more heterogeneities they encounter and thus their complexity increases. Thus, the later portions of the seismogram may be considered as a result of some kind of averaging over many samples of heterogeneities [2].

We conclude then, that the measured displacements of coda waves result from the superposition of many partial waves which have propagated along different paths between the source and the receiver containing the complexity of the travel media. Each path consists of a sequence of scattering events.

1.2.3. Spectral content

In the bibliography, coda waves seem to cover a wide range from 1 to 50 Hz [18]. More extensively, they appear to have different characteristics and content in various frequency bands. This makes sense if we think that the earth's scatterers are not the same size and differ from path to path, transferring those differing characteristics to the Coda wave that passes through them.

<u>Frequency $< 1Hz$</u>

For frequencies $< 1\ Hz$, the progress the last years is slow because of the difficulty to isolate the attenuation effect on amplitudes from various other effects due to complex heterogeneity of the earth medium [18]. In other words, not only scattering takes place in this bandwidth but several other phenomena in different proportions, rendering the isolation of each process impossible for the time being.

Furthermore, in this spectral Bandwidth, the Coda waves are masked by the arrival of ballistic waves [1], adding more complexity to our problem. To solve this problem though, several authors didn't consider the coda wave to initiate at the point mentioned earlier ($t_{coda} = 2t_s$) but after 10 seconds after the arrival of the S waves ($t_s + 10sec$) until 50 seconds after ($t_s + 50sec$). In this way they initiated the coda wave further along the waveform and got rid of a big part of the "Masking" caused by the ballistic waves [11, 13].

.

<u>Frequency $> 1Hz$</u>

At Higher frequencies, as mentioned above, coda waves present a dependence on the wave path [2]. More extensively, in a research the authors found that in frequencies from $1.5 - 3\ Hz$ from quarry blast signals obtained by in the early part of the record are strongly affected by surface waves and this characteristic disappears for the later part of the seismogram [20]. They used this characteristic as a way of discriminating of blasts and earthquakes.

At frequencies $> 10\ Hz$, the attenuation value was found to be high and a possible explanation was that the signal was not composed from backscattered surface waves but by backscattered body waves generated from inhomogeneities in the lithosphere [3]. This was supported by some works [$e.g.\ 2$] and contradicted by another work [22] where the authors studied Lunar coda waves and supported that in terrestrial codas the band where the scattering mechanism is prevalent is $1 - 25Hz$.

We begin to see in this spectral range that the Scattering begins to be the primary source of Seismic coda wave production. Indeed, in the frequency band of $25 - 35\ Hz$ another study suggested that the Coda waves would be less contaminated by surface energy [30]. This is the reason we also selected the frequency band of $2 - 16Hz$ to conduct this work. Apart from indications from the bibliography to support this choice, this band had the highest signal energy as shown in its power spectrum density.

Generally, a dependence of the coda-wave attenuation with frequency is proven [24] and it is a fact attributed to earth's inhomogeneity due to the large magnitude scale of earth's scatterers as mentioned earlier. The same frequency dependence was found and studied by other authors [$25, 26, 27$] where an attenuation model with a frequency dependant law was proposed. More extensively, the attenuation was dependant on the frequency following a Power law form.

In another study with the same concept, the author divided the coda signal into particular frequency bands and found that the shape and type of curves is controlled by the scattering and attenuation volume sampled by the coda waves [44].

1.2.4. <u>Effect of source dimensions and seismic momment</u>

In a research conducted [4] it was shown that if the source dimensions increase, the characteristic length of the waveform generated is bigger and thus the peak of the spectrum (Maximum generated frequency) shifts to lower frequencies [4]. While the form of the spectrum and thus the coda waveforms consistency, was independent of the seismic moment.

Also, in the same work, they indicated that that for larger events, the peak of the spectrum shifts to lower frequencies. The reason was that with increasing source dimensions, the seismic moment increases as well, and thus the same rule is applied.

This was proven afterwards by another study [31] where the authors found that the peak of attenuation is at peak for wavelength at 2 times the crack surface size. This phenomenon was attributed to resonant oscillation on the crack surface.

The important part here for us to keep, is that the consistency of the coda waves for the frequency bandwith we selected $(2 - 16Hz)$ depends only to the wave path and not the earthquake magnitude that generated the primary and secondary waves that got scattered into coda waves. In any case though, the events we selected had a large magnitude $Ml > 5.3$ In order to have a good quality and long signal.

1.2.5. <u>Effect of source depth</u>

If the depth affected somehow the generated coda wave, the only way this could hold true is that perturbations due to inhomogeneity of the part between the source and the receiver change with depth.

A study on this relation was conducted where the authors focused mainly on the measured impulse response at the surface before and after a slight perturbation of the velocity within a thin layer at depth. They concluded that the sensitivity depends mainly on (a) the level of heterogeneity of the model, (b) the lapse time, (c) the source receiver distance and the depth of the change [28].

Also another study found that attenuation decreases with depth [24], this indicated that the deeper part of the earth's crust is comparatively homogeneous to the upper part

So those studies by solving the opposite problem, verified again that coda waves exist because of the fact that earth is heterogeneous.

1.3. Initiation and end

As all the physical events,
They last only for so long.
As long as a particular
Property exists.

According to the bibliography [59], if t_{sp} is the time window between the arrival of primary (P) and secondary (S) waves and t_p, t_s is the time arrival of (P) and (S) waves respectively, the temporal decay of coda wave energy initiates for travel time $> 2t_{sp}$.

This means that the Coda waves initiate at $t_{coda} = 2t_{sp} = 0\ sec$ and they finish when the signal to noise ratio falls in the range of $\frac{Signal}{Noise} = 1 - 3$ as shown in $Fig.\ 2$. It must be noted is that noise is the background recording before the arrival of the seismic event $t < t_p$ assuming that there is no pre-seismic event in the recording.

The above numbers are verified by a study that showed that for travel time $> 2t_{sp}$ the vertical to horizontal kinetic energy ratios are stabilized in the coda part of the earthquake [5], which is a characteristic of coda waves as we saw earlier.
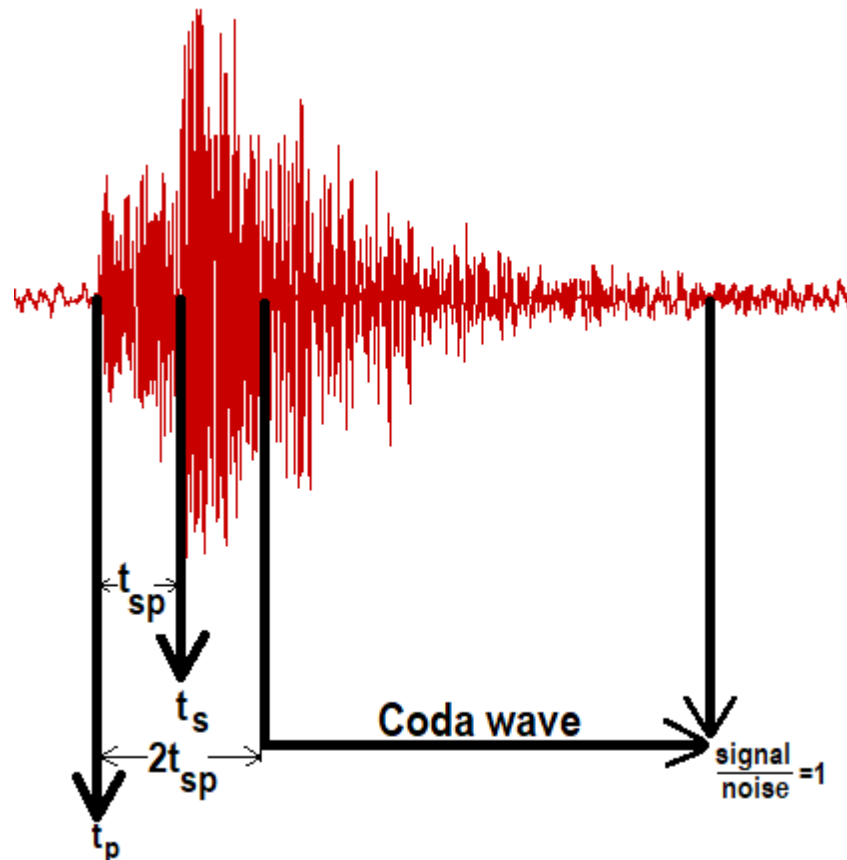
Figure 2: The coda wave initiates at $\boldsymbol{t_{coda} = 2t_s}$ where $\boldsymbol{t_s}$ is the time between the arrival of the P and S-waves and stops where the signal to noise ratio is close 1

1.4. Coda wave theories

Although a straightforward deterministic interpretation is difficult because of the extreme sensitivity of those waves to the complex inhomogeneities they encounter, a lot of work is ongoing. The theories are constantly changing to model as efficiently as possible the real complexity of earth's subsurface.

Untill now, the main mechanisms concerning the Coda wave propagation and interaction with the medium for the time being are the scattering, diffusion and absorption.

1.4.1. Coda wave generation as a scattering process

In order to have scattering you need to have scatterers and there are two main models according to the nature of their distribution within the medium. The wave medium may be homogeneous or heterogeneous.

The first is the backscattering wave theory where the coda is formed by the superposition of single-scattered wavelets caused by homogeneously distributed inhomogeneities [2, 29]. Because of the nature of scattering in this case, which is a weak process, loss of seismic energy can be neglected which is very helpful in the complexity of the model. The scattering process and the energy loss induced by it, control the shape of the seismic envelope and the spatial distribution of the energy [13].

If in the other hand, the medium is considered inhomogeneous, then we may model this problem as a space with average characteristics (Velocity, density or Lame parameters) where deviations from those mean values produce random heterogeneities. This type of problem is extremely complicated and the scattering field is treated as a continuous medium where inhomogeneous wave equations have to be solved. Also the energy loss in this case is bigger and it cannot be assumed negligible.

Both models though, despite having different formulation, lead to similar formulas. Also In any given system, not only one of the models is applied each time, a combination is considered in most of the cases. A study conducted about the energy distribution inside the coda waves [13] showed that within three 15-second windows, the energy $[log(x^2)]$ of the seismic envelope was concentrated in the first window for weak scattering which represents the first model and in the two other widows for stronger scattering which represents the second model.

There are also 2 different types of scattering according to the amount of scattering the wave subdues to. Single and multiple scattering.

Single scattering

In the beginning, Geophysicists modeled coda wave production via the simplistic single-scattering assumption where the scatterers were -uniformly distributed and point-like. Each coda wavelet was a single-scattered ballistic wave. The supporters of this theory supposed an inverse square law for the geometrical spreading of seismic energy in a 3-dimentional space and thus, obtained the S-coda power decay dependence on the lapse time [2].

Following this model, several investigations have been conducted in order to test if this model explains adequately the coda-wave characteristics. In one study, space-time dependence of the energy density of scattered waves in a 3-D space was modeled and that explained adequately how scattered energy becomes homogeneously distributed as lapse time increases, which is an actual coda wave characteristic as we saw earlier [34, 35, 36]. Later, another study managed to synthesize 3-component seismogram envelopes using the Born approximation in inhomogeneous random structure following the same manner and the results were quite realistic [14] (The Born approximation has the advantage of the independence of the effect of shape of the scatterer in a scattering problem).

One major problem with single-scattering problem though, is that it violates the energy conservation due to oversimplification of the problem (caused by the born approximation). This model assumes that earthquake source and the seismic station are located at the same point in an unbounded homogeneous and isotropic medium containing a uniform spatial distribution of inhomogeneities. Attempts to make the model more realistic were tried by considering a finite distance between the source and the receiver [37].

Multiple scattering

Following the same manner, multiple scattering was recognized as a possible model [2]. At a theoretical level and at long lapse times, the coda amplitude decay was studied based on the assumption of a multiple scattering process [38]. Another theoretical study about the multiple scattering process was conducted [39,40] and a respective numerical simulation via Monte-Carlo was later adopted [41].

After all the modeling, the fact that coda waves compose of multiply scattered waves was verified as it was found from slowness analysis that each of the numerous partial waves follows a different path and not a linear one from the source. Also the Gaussian nature of coda phases was unveiled by phase analysis in the same study [1]. Multiple scattering assumes secondary scattering (or higher order) to occur and the seismic energy transfer to be a diffusion process.

However, these derivations about multiple scattering processes are based again on the inverse square law for geometrical spreading and the total energy is not again conserved. This issue was partially solved in a study where the author simulated numerically the space-time distribution of energy density by using again the Monte-Carlo simulation and he also adopted the energy conservation law, showing the partition of scattered energy into different order-scattering as a function of lapse time [42].

Later other models more specific and realistic models were investigated to simulate the inhomogeneity characteristics of certain regions. For example a hybrid model was proposed where a large impedance contrast plane was embedded in the scattering medium to interpret the reflected S-wave phase [43].

1.4.2. <u>Coda wave generation as a diffusion process</u>

The second proposed process of seismic coda generation is the seismic energy transfer as a diffusion process which was proposed and studied by several other authors [2, 22, 23] but not in the same extent as the scattering process.

But when does the diffusion process is more dominant? This question was answered in a study about lunar codas. The authors concluded that If x^* is the attenuation distance, which is the average distance seismic energy travels before attenuation takes place and mean free path L which is the distance before scattering takes place, a discussion of the diffusion scattering model, indicates that, if $\frac{x^*}{L} \gg 1$ then diffusion scattering is more appropriate. On the other hand, if $\frac{x^*}{L} \ll 1$ then single scattering is the appropriate model [22]. So the answer in short, is that it depends on the distance from the source.

1.4.3. <u>Coda wave generation as an absorption process</u>

The kinetic energy of the earthquake turns into mechanical energy by moving energy particles from their positions. But because the earth deviates from the ideal harmonic oscillator model, due to friction, some of the energy is absorbed by the molecules and is transformed into heat.

More extensively, propagation of short-period S-waves through the crust is strongly controlled by intrinsic absorption which is also responsible for the exponential decay as a function of time [13]. It constitutes though a small degree of the mechanisms that take place to generate coda waves.

1.5. Use of coda waves

1.5.1. <u>Information about the medium</u>

It is of great importance to determine the type of the medium considering the signature found in seismic responses. This scenario is rendered viable with the use of coda waves. They are unaffected by earthquake magnitude and distance and thus they contain pure data about scattering effects, without being corrupted by absorption [11, 30]. Also the coda waves are not affected by source radiation patterns because the scattering process averages the radiation over the focal sphere.

Due to those characteristics, a lot of work has been conducted to correlate the relationship of coda waves with the earth's inhomogeneities (scatterers). This is also the largest portion of their application and use.

The dependence of coda waves to local crust composition motivated some authors to use a statistical treatment with a small number of parameters, which is proved to be a good way to characterize the average properties of the heterogeneous medium [2]. There have already been also several trials to characterize media in terms of stochastic heterogeneities using amplitude and phase fluctuations [47]. However, there is a strong dependency of those fluctuations to the propagation path and thus the measured results display a different pattern following the appearance of the media.

A typical application performed by many authors, is the study of the strength of coda wave attenuation in several places around the globe. In this way they attempted to correlate the attenuation with the characteristics of the medium through which the seismic wave propagates [24]. Another example is a study where the authors analyzed the patterns of phase and amplitude variations of seismic waves across a seismometer array on a statistical basis. In their attempt they tried to determine the statistical distribution of the heterogeneities under the array [46].

In the same context and local scale, several authors have indicated that the local site characteristics may be a major source of great scatter and possible bias in attenuation measurements [18]. Since the site effect may vary greatly with the path connecting the source and the receiver, the authors used single station method and using deep earthquake sources to minimize the number of site effects and biases. It must be noted that [18] didn't find any change of Coda attenuation with depth for the same station in the ground and in a 100m borehole.

1.5.2. <u>Information about the earthquake source</u>

The difference of Coda amplitudes among the stations for a particular earthquake is found to be caused solely by site factors. This makes sense as coda excitation is dependent on local geology and thus ambient site factors.

Some studies have used the characteristic mentioned above and devised a methods to extract info about earthquake source from the coda of small local earthquakes. They were based on the assumption that power spectrum of coda waves of local earthquakes is only a function of time measured from the earthquake origin time and also independent of the distance and the details of the wave path to the station in terms of signal

homogeneity. The latter means that the coda energy is homogeneously distributed though the spectrum due to the averaging it is subdued to from encountering scatterers. (for distances less than 100 km) [7,45].

1.5.3. <u>Information about tectonic activity</u>

The applications of coda waves have been extended to the point of monitoring tectonic activity too. Continuous monitoring of the coda tails in a station may detect stretching of the seismic signal. As we mentioned before, the attenuation is characteristic for each station (site effect).

Stretching of the coda tail bodes changes in the media texture under the station or in other words, small velocity changes. This correlates with tectonic activity in the region and stress accumulation [5, 27] that causes the pressure and thus density of the material to deviate from its usual values. In the same context there have been studies reporting that temporal change of the coda-wave decay before or after major earthquake events are directly correlated [48,49]

Another author studied the scattering of elastic shear waves by a zonal distribution of cracks which is a realistic case a fault fracture zone. The study resulted in how the geometrical characteristics of the crack distribution and frictional characteristics of the crack surface may affect the attenuation and dispersion of incident waves and the amplitudes of the transmitted and reflected waves from the zone [45]. This could be a possible way of monitoring temporal changes in the fault-crack distribution via the scattered way that propagate through them.

Concluding, Coda wave analysis is proven be very powerful tool for the investigation of source spectrum and site effects as well as the evaluation of the tectonic activity and crustal inhomogeneity.

2. Statistical treatment and Principles of Non Extensive Statistical Physics (N.E.S.P.)

The statistical treatment of P and S waves of a given seismogram is not easy as their properties are determined by the particular nature of the path between the seismic source and the receiver.

The coda-part of the earthquake though, is composed of numerous backscattering wavelets caused by the earth's complex lateral heterogeneity [7] as mentioned earlier. If those numerous heterogeneous parts of the earth's crust generate secondary waves, the total of the backscattering waves composing the coda wave will be a superposition of these secondary waves and may be considered as a sum of many independent small events.

Thus, due to this averaging an entirely statistical treatment can be applied.

2.1. The unveiling of Earth's complex structure-Fractality

The greatest part of the earth's crust inhomogeneity is too complex to be handled by deterministic methods. A more realistic scenario is that of random scattering whose effects can be considered as a statistical average [50]. This statistical way of thinking led authors to develop new inversion methods of coda waveforms from local earthquakes, in order to estimate the inhomogeneous spatial distribution of scattering intensities in the crust and uppermost matle [51].

There were created statistical models that tried to simulate seismic wave characteristics. In one of those cases the authors simulated envelopes of scalar waves. The simulation involved Monte-Carlo simulation of the wave-energy transfer [52]. The study was tested for 3 different radiation pattern autocorrelation functions of inhomogeneities: Gaussian, Power law and a Mix of the above and they tried to find which model could quantitatively reproduce the 2 most characteristic features of the Real S-wave envelopes of close-proximity

earthquakes. The first is the broadening of the primary wave group and the second is the Coda-part of the waveform.

The outcome was that the fractal case reproduced qualitatively in the best manner the observed wide-band behavior. It was thus considered then the best reasonable representation to describe the gross properties of the earth medium.

2.2.   Principles of N.E.S.P.

2.2.1. The non-Additive Entropy

The theory we stepped on in order to conduct this work is based on the concept of entropy. The formalism of non-extensive statistical mechanics can be regarded as an embedding of ordinary statistical mechanics into a more general framework. The well known and widely applied Boltzmann-Gibbs entropy S_{BG} is generalized into the Tsallis entropy S_q introduced by Tsallis [53] and is given by:

$$S_q = k_B \frac{\sum_{i=1}^{W} p_i^q}{q-1}$$

Where k_B is the Boltzmann's constant, p_i is a set of probabilities, W is the total number of microscopic configurations and q is the entropic index for $q = 1$ the Tsallis entropy reproduces the Boltzmann-Gibbs entropy:

$$S_q \xrightarrow{q=1} S_{BG}$$

As Tsallis proposed, we could empirically deduce S_q by simple physical principles and multifractal ideas concept. The entropic index "q" inroduces a bias in the probabilities. Given the fact that $0 < p_i < 1$, we have that

$$p_i^q > p_i \quad if \quad q < 1$$
$$p_i^q < p_i \quad if \quad q > 1$$

Therefore, $q < 1$ enhances the rare events with $p_i \to 0$, whereas $q > 1$ enhances the more frequent events with $p_i \to 1$. Following the same context, it is natural to introduce an entropic index based on p_i^q. The entropic form must be invariant under permutation and the simplest expression that is consistent with this, has the form

$$S_q = F\left(\sum_{i=1}^{W} p_i^q\right) \quad (1)$$

Where $F(x)$ is a continuous function. The simplest form of $F(x)$ is a linear one, leading to

$$S_q = C_1 + C_2 \sum_{i=1}^{W} p_i^q \quad (2)$$

As any entropy, S_q must be a measure of disorder leading to $C_1 + C_2 = 0$, and thus, from Equations $(2), (3)$ we lead to

$$S_q = C_1\left(1 - \sum_{i=1}^{W} p_i^q\right)$$

In the limit $q \to 1$, the entropic form S_q approaches the Boltzmann-Gibbs expression and the simplest way for this to happen is when

$$C_1 = \frac{k_B}{q-1}$$

The index "q" is the degree of non-additivity that accounts for the case of many non-independent, long interacting subsystems, and memory effects $[53, 59, 60]$. In the majority of the studied systems, the non-additivity index, "q", seems to reflect some multi-Fractality to the system.

The main difference of S_{BG} and S_q entropy functionals, is that they are said to be Additive and Not additive respectively. Additive entropy functional means that for two probabilistically independent subsystems constituting a main system A, B, the entropy of the whole system equals with the sum of the entropies, which is the case for $q = 1$. Non additive entropy functional violates this property.

$$\textit{Additive} \qquad S_{BG}(A + B) = S_{BG}(A) + S_{BG}(B) \qquad (2.1)$$

$$\textit{Non Additive} \qquad S_q(A + B) = S_q(A) + S_q(B)\frac{1-q}{k_B} \qquad \forall(q \neq 1) \qquad (2.2)$$

Where $(1 - q)$ can be considered to be the measure on Non-additivity of the investigated systems

Apart from additivity, there is another property that makes systems distinct in terms of entropy. This property is the thermodynamic concept of Extensivity. A system with a large number of elements "N" is called extensive if its entropy is asymptotically proportional to "N". Otherwise, the system is called non extensive.

Contrary to additivity, extensivity depends and on the entropy functionals and on the (possibly existing) correlations of the system. For example, a system with independent or weak correlated elements has extensive additive entropy S_{BG} and non extensive non additive entropy S_q. To the contrary, in a strongly correlated system,

the additive entropy S_{BG} can be non extensive whereas the non additive entropy S_q can be extensive for a certain value of q. There are also probabilistic systems, where S_q is non extensive for every value of q.

2.2.2. __The Additive Entropy__

It was in $1870's$ that Ludwig Boltzmann introduced the first form of standard statistical mechanics. Thirty years later, the first objections began to rise. The case was that the foundation of Boltzmann's statistical mechanics was insecure from it's first principles as the whole work is based on hypotheses concerning the constitution of matter [54].

More specifically, not all the systems in nature can be described by Boltzman's statistical mechanics as the formula fails for complex systems. The information tool we will use in this work and that is generally used is Entropy.

The first entropy formula that was found and worked for the absolute majority of the systems known (simple and continuous ones), was the Boltzman-Gibbs one, which for W discrete states is:

$$S_{BG} = k \sum_{i=1}^{W} p_i \, ln p_i \quad (2.3)$$

Where k>0 and as stated by the normalization statement,

$$\sum_{i=1}^{W} p_i = 1 \qquad (2.4)$$

In the case of equal probabilities, meaning that $p_i = \frac{1}{W}$, the formula becomes

$$S_{BG} = k ln W \quad (2.5)$$

Equation (2.3) has an interesting property. In a system composed of two sub-systems probabilistically independent with numbers of states W_A & W_B respectively and where the joint probabilities fulfill the factorization statement

$$p_{ij}^{A+B} = p_i^A p_j^B \quad \forall \, (i, j)$$

The entropy S_{BG} is additive, and thus equation (3.1) is satisfied. last but not least, the optimization of equation (3.3) under eligible constrains, results, for a system in thermal equilibrium with a thermostat temperature "*T*", at the named 'B-G Factor of weight'.

$$p_{i=} \frac{e^{-\beta E_\iota}}{Z_{BG}} \qquad (2.6)$$

With

$$\beta \equiv \frac{1}{\kappa T} \qquad (2.7)$$

And

$$Z_{BG} = \sum_{j=1}^{W} e^{-\beta E_j} \quad (2.8)$$

Boltzman's entropy as we mentioned earlier is not a universal functional that works for all kinds of systems, but it is a concept that has to be revised for every different class of system. It works adequately in the case of simple continuous systems, it needs to be modified in the case of complex systems and there are also systems where the theory does not work at all. This is the logical outcome of the fact that the theory is a human intellectual construct and thus there will always be the human error abating the area of validity of the theory.

2.2.3. <u>Expanding The area</u>

The generalization f B-G statistical entropy was accomplished using a quite different metaphor, the 3 simplest differential equations were combined and then by taking advantage the concept of linerarity, the combination of the two parameters from the 3 differential equations were fused into one, the q-parameter.

The simplest differential equations are said to be:

$$\begin{cases} \dfrac{dy}{dx} = 0 \;,\; y(0) = 1 & \text{with solution } y = 1 \quad (2.9) \\[2mm] \dfrac{dy}{dx} = 1 \;,\; y(0) = 1 & \text{with solution } y = 1 + x \quad (2.10) \\[2mm] \dfrac{dy}{dx} = y \;,\; y(0) = 1 & \text{with solution } y = e^x \quad (2.11) \end{cases}$$

Unifying the equations (3.9), (3.10), (3.11), we get:

$$\frac{dy}{dx} = a + \beta y \;,\; y(0) = 1 \xrightarrow[\text{with linearity, } a,\beta \to q]{}$$

$$\to \frac{dy}{dx} = y^q \;,\; y(0) = 1 \;,\; q \in R \quad (2.12)$$

With solution

$$y = [1 + (1-q)x]^{\frac{1}{1-q}} \equiv e_q^x, \quad e_1^x = e^x \quad (2.13)$$

And its inverse

$$y = \frac{x^{1-q} - 1}{1 - q} \equiv ln_q x \;,\; x > 0, \qquad ln_1 x = ln x \quad (2.14)$$

After this work, we managed to create two vital components of Tsallis Non Extensive Statistical Mechanics. Equation (2.13) is named q-exponent and Equation (2.14) is named q-logarithm.

The main characteristic of the q-logarithm is that contrary to the normal logarithm, it is non-additive. This happns due to the mixing terms that appear when we try to add two q-logarithms of two different terms A,B.

$$ln_q x_A x_B = ln_q x_A + ln_q x_B + [\![ln_q x_A ln_q x_B]\!] \quad (2.15)$$

where

$$[\![ln_q x_A ln_q x_B]\!] = Mixing\ terms$$

The property of Equation (2.15) is called Pseudoadditivity.

The Generalization of B-G statistical mechanics as one would expect, can derive from replacing the standard exponential and logarithm forms with the q-generalized ones.

The above is verified by a study that showed that for travel time $> 2t_s$ the S/P energy ratio is stable in the coda part of the earthquake and the vertical to horizontal component kinetic energy is stabilized [5], characteristics that hold true for Coda waves.

2.2.4. **The non-additive entropy S_q**

Through the metaphor presented above, we replace the normal logarithm with the q-logarithm and so we obtain the generalization of Equation (2.5) for equal probabilities:

$$S_q = k ln_q W \quad \text{with} \quad S_1 = S_{BG} \quad (2.16)$$

And for the general case of arbitrary p_i (not equal probabilities) applying Equation (2.14) to the Equation (2.5) for equal brobabilities yields:

$$S_q = k \frac{1 - \sum_{i=1}^{W} p_i^q}{q - 1} \quad (2.17)$$

It is also clear that the pseudoadditivity property of the q-logarithm in Equation (2.15) comes from the q-generalized entropy. This is easily verified if we add the generalized entropies of two independent systems A,B. where the joint probabilities fulfill the factorization statement:

$$p_{ij}^{A+B} = p_i^A p_j^B \quad \forall \, (i,j)$$

We have then

$$\frac{S_q(A + B)}{k} = \frac{S_q(A)}{k} + \frac{S_q(B)}{k} + \left[\!\left[\frac{S_q(A)}{k} \frac{S_q(B)}{k} \right]\!\right] \quad (2.18)$$

Where $\left[\!\left[\frac{S_q(A)}{k} \frac{S_q(B)}{k} \right]\!\right]$ =Mixing terms. This is the property that makes S_q for $q \neq 1$ to be non-additive. The generalized entropy functional in Equation (2.17) is also valid for continuous variables by changing the sum to integral:

$$S_q[p] = k \frac{1}{q-1} \left(1 - \int p(x)^q dx \right), q > 1 \quad (2.19)$$

Which functional in the limit $q \to 1$ also converges to the ordinary Boltzmann Gibbs entropy:

$$S_q[p] = k \int p(x) \ln p(x) dx$$

2.2.5. Entropy maximization

Let us consider the maximization of S_q in Equation (2.19) with conditions:

$$\begin{cases} \int p(x) dx = 1 \\ \int P^q(x) U(x) dx = U_q \end{cases} \quad (2.20)$$

Where

$$P^q(x) = \frac{P^q(x)}{\int P^q(x) dx}$$

Is called the Escort probability, $U(x)$ is the function under study which describes the systems' behavior and U_q is called q-average. In the case of parabolic function $U(x) = x^2$, U_q becomes a generalized variance σ_q^2 which responds to the intensity of the fluctuations [???].

3. Data selection

The Data Were selected from 2 Datasets. One in South Aegean, recorded from H.S.N.C. network, and one in northern Italy, recorded by the I.N.S.I.E.M.E. Network in the south Apennines.

3.1. Data acquisition stations

3.1.1. South Aegean data set

The data for the first part of the work, are taken from APE, ARG, CHAN, KNDR, KRND, KSTL, KTHR, MHLO and NHS1 stations of the Hellenic seismological network [55] and the seismometers used are Guralp-$3ESPC$ Weak motion seismometers with a frequency response of $120s - 50Hz$ and a sample frequency of $100Hz$.

We used 4 Major earthquake events to perform our analysis:

1. 10/12/2013 13:11:53, Mag.=6.2, Recorded by APE,ARG KRND,MHLO,NHS1
2. 06/15/2013 4:11:01 Mag.=5.8, Recorded by ARG,CHAN,KSTL,KTHR,MHLO
3. 04/16/2015 18:07:44, Mag.=6.1, Recorded by APE,ARG KRND,KSTL,MHLO,NHS1

Figure 3: The earthquake events used in the south Aegean dataset.

As mentioned earlier, their magnitudes are large enough to acquire good quality of signal and a long coda wave recording. We excluded the recordings where the coda wave was either clipped or very noisy. So the stations mentioned above represent the best quality recordings.

3.1.2. South Greece Complexity

The area of southern Greece is characterized by its high complexity. It is strongly affected by geodynamic phenomena due to the convergence of the African and European plates [63]. Southern Greece is the most seismically active part of Europe and fault movements produce vertical changes in the height of the land, commonly observed by local changes in sea level.

More extensively, The Mediterranean tectonic plate is being subducted below the Aegean Sea. The melting of the plate produces molten rock, which rises to the surface as the South Aegean volcanic arc which acts as a velocity boundary. This makes the region north of the arc to expand, forcing Crete southward and producing earthquake events.

In addition, the Anatolian plate is pushing eastward, separated from the Eurasian plate by the North Anatolian fault and its extension, the North Aegean fault zone. Also, the Mediterranean plate subducts along a major thrust fault and melts at a depth of 100 km to feed the active volcanoes and faults provide channels for surface water to descend deep in the Earth and rise as hot springs [64].

The complexity hidden underneath the surface of this site renders it ideal to check our theory.

3.1.3. **South Appenines Records**

The data for the second part of the work, are taken from INS1,INSx stations of the "SIR-MIUR Project INSIEME-Broadband seismic network in Val D'Agri (Southern Italy)" seismological network [61].

This selection was such because those 2 stations are positioned in different depths. INS1 station is positioned on ground level while INSX station in positioned in a borehole 50m underground. In the same time, those stations are on the same coordinates with only 30m distance, which in our case is irrelevant as the earth's scatterers have a much larger scale length and the earthquakes studied occurred very far away.

The seismometers used are IRIS-Trillium Compact Seismometers with a frequency response of $120s - 50Hz$ and a sample frequency of $250Hz$.

For this work we used 4 seismic events occurred in Italy and 2 seismic events occurred in Greece.

1) 26/10/2016 Ml=5.5 Central Italy.
2) 01/11/2016 Ml=4.9 Central Italy.
3) 18/01/2017 Ml=5.5 Central Italy
4) 16/10/2016 Ml=4.8 Greece
5) 16/10/2016 Ml=4.0 Greece
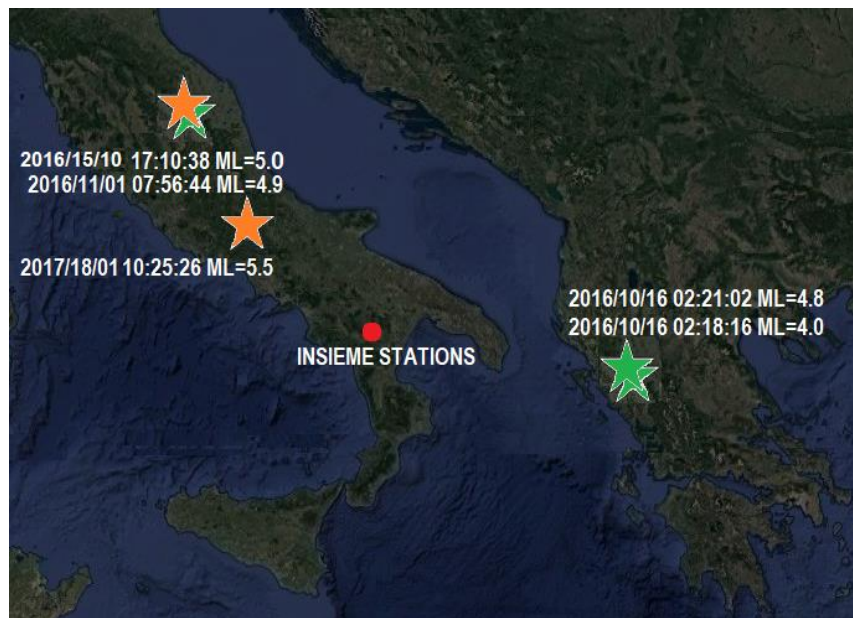
Figure 4: The earthquake events used in the INSIEME dataset.

3.1.4. The complexity of the Southern Apennines

The south Apennines fold-and-thrust belt is a circum-Mediterranean orogeny, where the complex tectonic and stratigraphic imprint is preserved and enhanced every year due to the continuous collision between African and European plates.

More extensively, the structural geometries characterizing the southern Apennines, as well as the out-of-sequences thrusting and the basin networks due to differential erosion and fracturing, have high degree complexity as they have resulted from complex deformation and depositional history [65,66,67,68].

Like the Southern Greece's case, it is an ideal site to check for complex structures through our theory. We expect in both sites the complexity of the earth's crust to be projected onto the Coda waves.

3.2. Coda wave selection

As mentioned in the introduction, only a certain part of the seismogram has the certain characteristics needed to be called Coda Wave. Using the Bibliographic information, we will isolate the coda part with computational methods.

3.2.1. Coda wave initiation

The data analysis in this work were conducted with the use of Matlab© and Dimas softwares. The first part is the selection of the coda wave. To achieve this, we use the principles presented in the first chapter.

As mentioned in the first chapter, the first step was to find the time interval between the arrival of the P and S waves. This was a time window equal to time t_{sp}. We slided that window it for time equal its length so that the end of that slided window is in $t = 2t_s$ and thus, the initiation of the Coda wave according to the bibliography.

The coda part of the earthquake waveform is the part for $t > 2t_{sp}$. This process can be easily understood in Figure 3. Below:
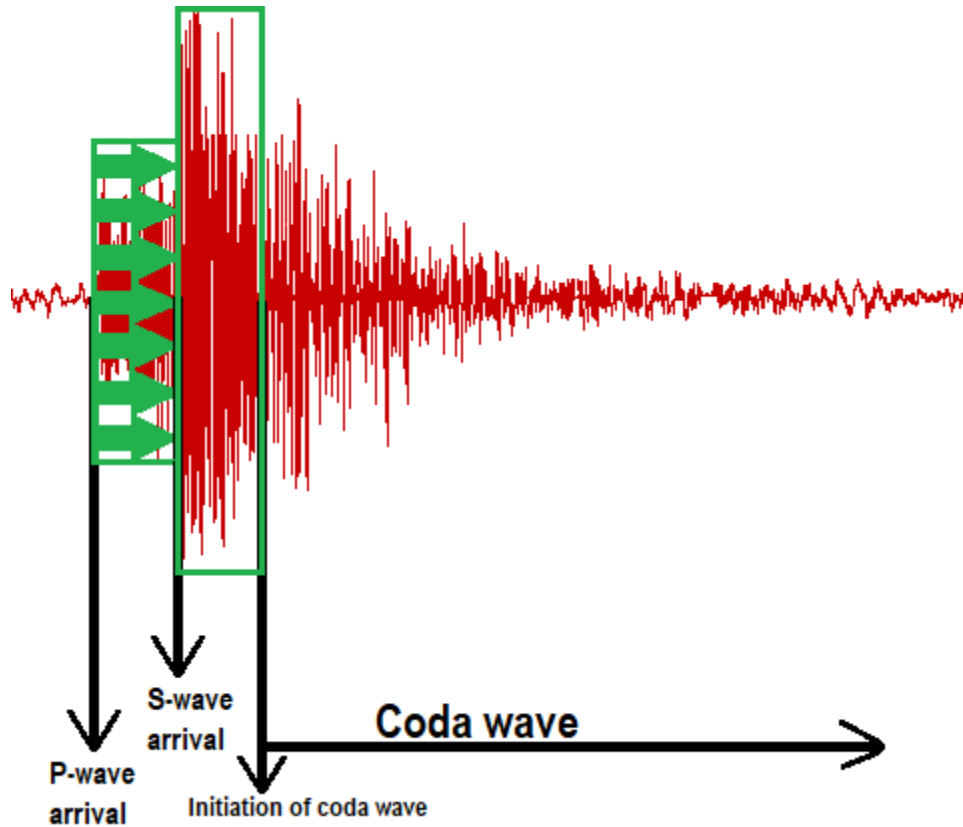
Figure 5: A window was selected with length equal to the time between the arrival of P and S waves(Green box). The window is slided for time equal its length.The end of the slided window composes the Beginning of the coda wave.

The process explained above was conducted in Dimas software and the Coda selected was very long (>10 minutes). Following, with the Sliding window method, we calculated the ending of the Coda wave.

3.2.2. <u>Coda wave ending</u>

We defined the ending of the Coda waveform, as the point where the $\frac{Signal}{Noise}$ ratio reached the value 3. We achieved that by making an algorithm in Matlab (given in the appendix), which with continuous iterations calculated the signal to noise ratio for the whole length of the waveform beginning at the point $t_{Coda} = 2t_{sp}$. The method worked as following.

<u>Noise window</u>

We selected a time window before the arrival of the P-waves which represent the noise fluctuations of the signal. The noises' window length "t_{noise}" varies between $1 - 3\ minutes$. The selection of this time length

was such, because we observed that the averaging of the noise windows comes to saturation after~$0.2\ Seconds$. As shown in Figure 5 Below:
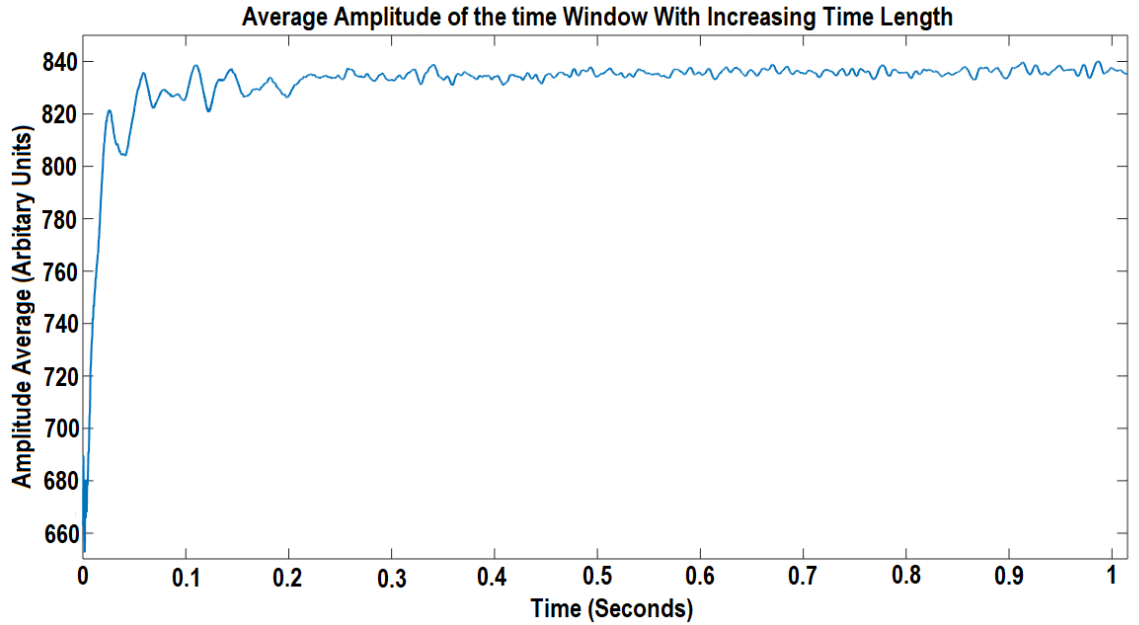

Figure 6: By increasing the time window we see that its average amplitude comes to saturation after around 0.2 Seconds

So we concluded that for $t_{noise} = 1 - 3\ minutes$ should be an adequate time frame in order to acquire the real average value of the noise fluctuations in each coda wave. Following, we found the average Amplitude value of the amplitudes "$\bar{N}$" within that noise window.

<u>Signal window</u>

After the noise window selection we selected a same length time window within the coda wave initiating at $2t_s$ and finishing at $2t_s + t_{noise}$. In the same manner, we evaluated the average amplitude value of the First Signal window "$\bar{S}_1$" and then we calculated Signal to noise ratio (SNR) for the First signal window:

$$SNR = \frac{Signal}{Noise} = \frac{\bar{S}_1}{\bar{N}}$$

With an iteration loop we do the same by sliding the Signal window by one count each time. Knowing that the sampling rate of the seismometer is $100Hz$, 1 count equals to $0.01\ Second.$ So the sliding window is $0.01\ Second.$ In each iteration "i" we calculated the respective signal to noise ratio:

$$SNR_i = \left(\frac{Signal}{Noise}\right)_i = \frac{\bar{S}_i}{\bar{\bar{N}}}$$

The loop stops at the nth iteration where:

$$SNR_n = \left(\frac{Signal}{Noise}\right)_n = \frac{\bar{S}_n}{\bar{\bar{N}}} = 3$$

In Figure 4 we can see the SNR values for the calculation of a coda wave.

It must be noted at this point that the amplitude value composing the data is voltage and its dimensions are in arbitrary units. We do not need to transform them to other units as we are interested in the fluctuations which entail the same information.
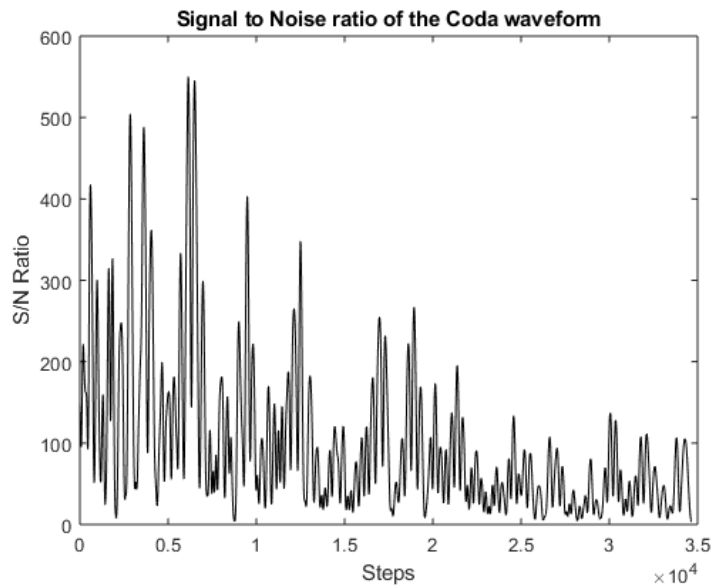
Figure 7: We see that the SNR value fluctuates greatly and drops to 3 after about 35000 iterations.
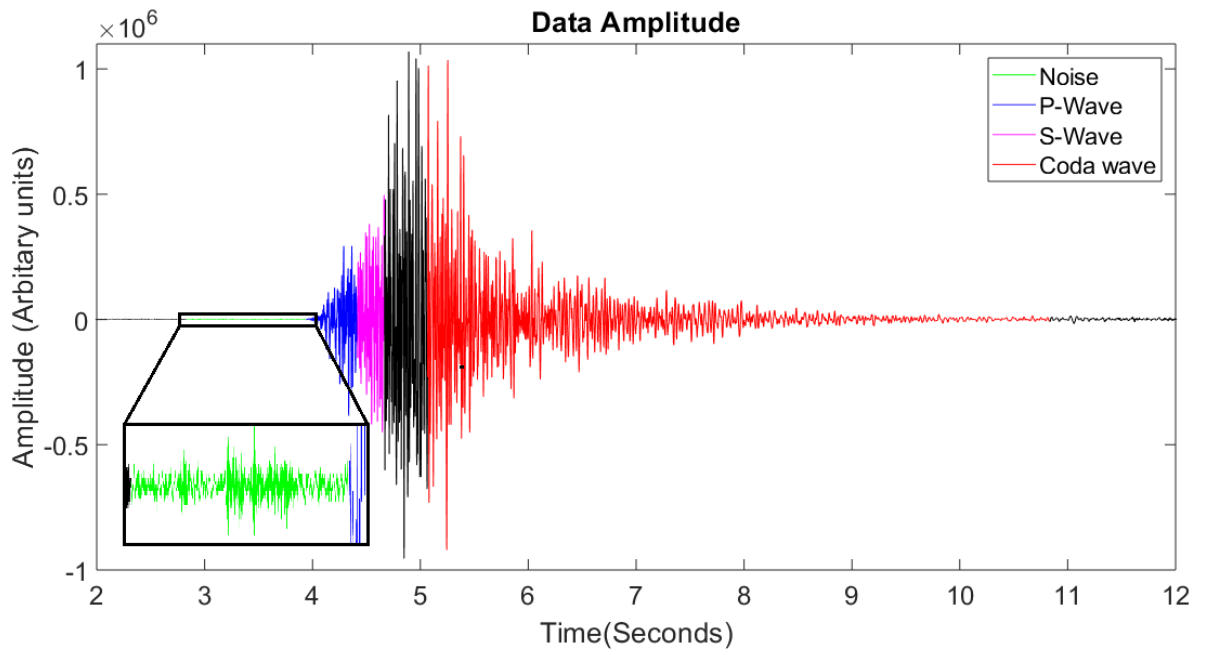
Figure 8: The selected coda wave (Red) after we evaluated the signal to noise ratio. we can also see the noise (Green) window selected as well as the Primary (Blue) and Secondary (Magenda) waves.
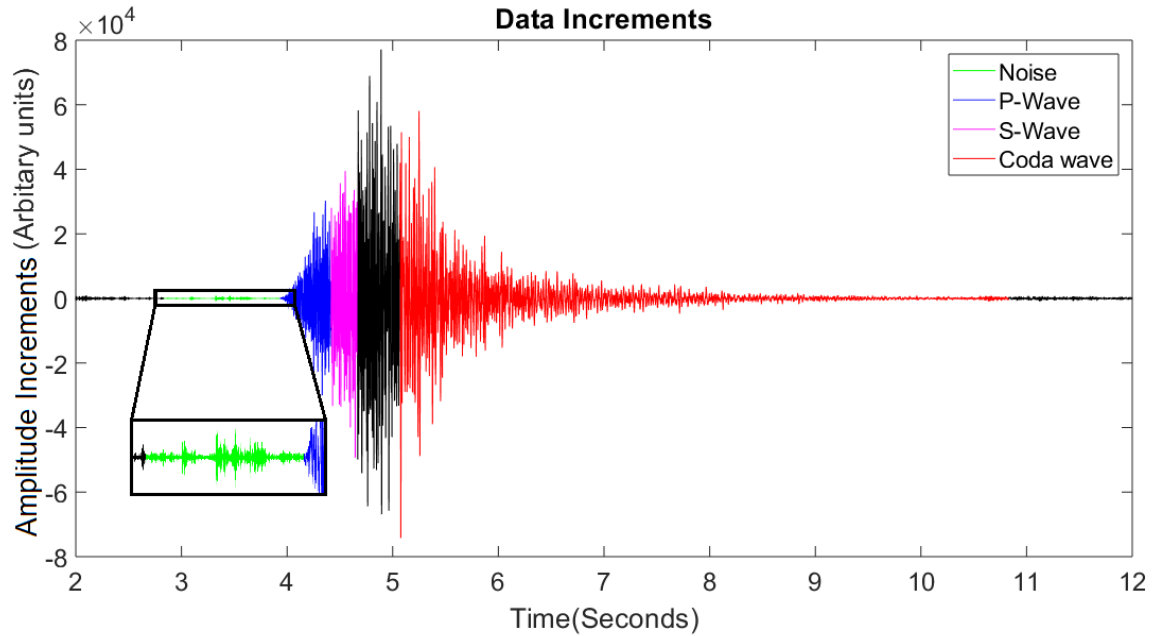
Figure 9: The Incremental values of the waveform of Figure. 8. we can again see the increments of the noise (Green) window selected as well as the Primary (Blue) and Secondary (Magenda) waves' Increments

Now we have our coda waves ready and set in place for the data analysis.

4. Data analysis

After having our coda waves cut and ready the next step is analysis. Following the non-extensive statistical physics approach, the probability distribution function of the increments of coda waves is investigated. We defined the function

$$X(t) = S(t + 1) - S(t) \quad (4.1)$$

Whereas $S(t)$ is the measured ground velocity in the East-West and North-South direction.

We proceeded by analyzing the normalized increments X(t) and constructing the Probability Density Function (PDF)p(x), normalized to zero mean and unit variance and introducing the variable $x = \frac{(X - \langle X \rangle)}{\sigma_x}$, With σ_x being the standard deviation of $X(t)$. This indicates that the PDF's associated with the normalized increments of

the measured coda waves, deviates from the standard Gaussian shape due to the existence of heavy tails and can rather be described by the q-Gaussian function of the form

1st EVENT	$q_{\text{East-West}}$	$q_{\text{North-South}}$
APE	1.86	1.84
ARG	1.83	1.82
KRND	1.88	1.87
MHLO	1.98	2.02
NHS1	1.60	1.59

$$p(x) = A[1 + B(q-1)x^2]^{-\frac{1}{q-1}} \quad (4.2)$$

In this point it must be mentioned that Incremental values show the evolution of changes in time series, since every point in the incremental series contains information of the present state of the measured value as related to the past, giving information on the existence of possible memory effects [61].

The q-parameters derived from the fitting of the observed data to Equation (4.2) are observed in the two following datasets.

4.1.   South Aegean Data Set

4.1.1. Coda Increments in the South Aegean Dataset Events

In this part of the analysis we fit the data of coda wave increments of the seismic events of the South Aegean data set to Equation (4.2) and found that $p(x)$ distributions deviate from the Gaussian shape and they can be satisfyingly explained by means of Non-extensive statistical mechanics.

More extensively, the q-values observed are shown in Tables 1,2,3 and respective figures of the two components (East-West and North-South) of each of the events are shown in Figures 9,10,11 Below.

Table 1: The q-values of the coda waves of the 1st seismic event as
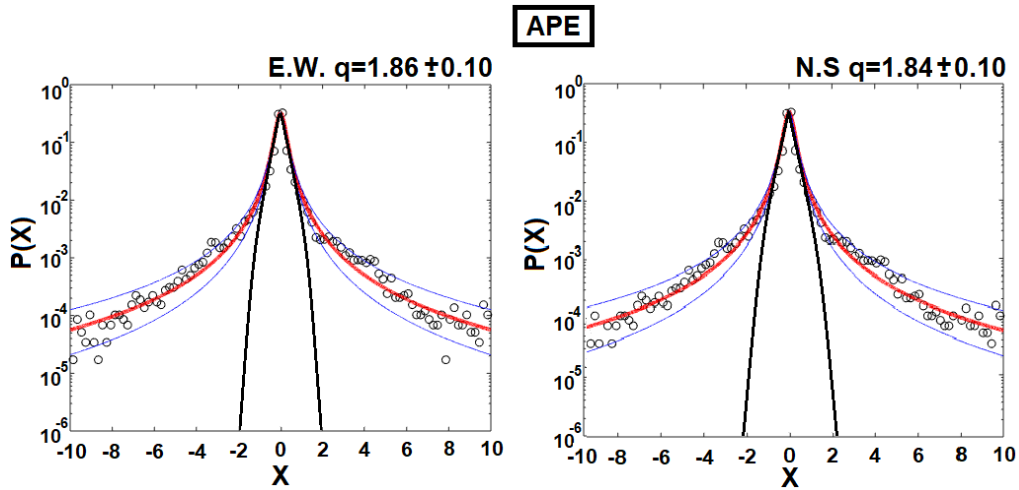Recorded by APE, ARG, KRND, MHLO, NHS1 stations of the H.S.N.C.

Figure 10: Incremental data of the coda waves from the 1st event recorded from APE station (Black circles) and the fitted Eq 4.2. (Red line). The 95% Confidence bounds give error $q_{err} = 0.10$ In the East-West component the q-value is $q = 1.86$ whereas in the North-South component is slightly less $q = 1.84$. In the image we also see the Gaussian Curve (Black line) which corresponds to $q = 1$.

2nd EVENT	q East-West	q North-South
ARG	1.35	1.37
CHAN	1.92	1.91
KSTL	1.92	1.92
KTHR	1.57	1.58
MHLO	1.89	1.86

Table 2: The q-values of the coda waves of the 2nd seismic event as Recorded by ARG, CHAN, KSTL, KTHR, MHLO stations of the H.S.N.C.
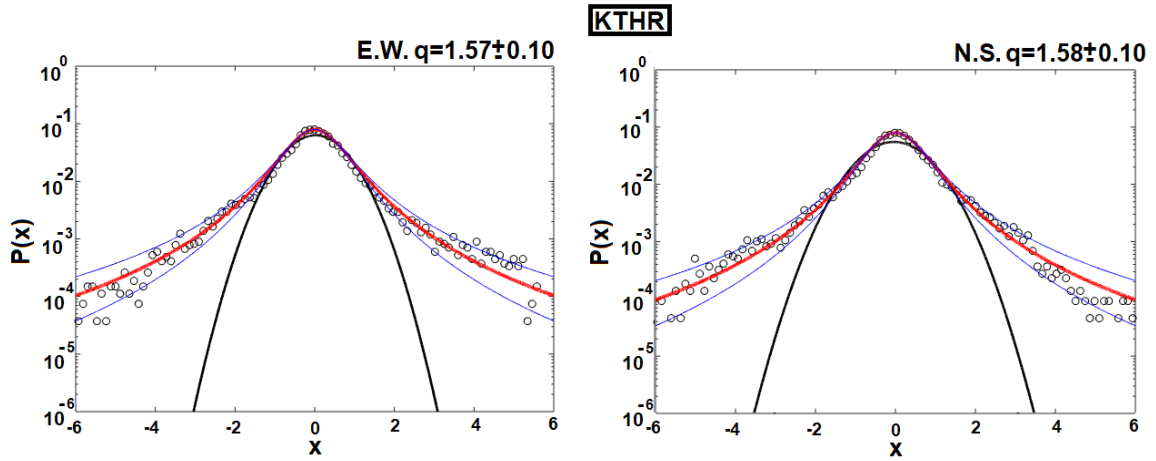
Figure 11: Incremental data of the coda waves from the 2nd event recorded from KTHR station (Black circles) and the fitted Eq 4.2. (Red line). The 95% Confidence bounds give error $q_{err} = 0.10$ In the East-West component the q-value is $q = 1.57$ whereas in the North-South component is slightly more $q = 1.58$. In the image we also see the Gaussian Curve (Black line) which corresponds to $q = 1$.

3d EVENT	$q_{East-West}$	$q_{North-South}$
APE	1.80	1.80
ARG	1.89	1.90
KRND	1.83	1.82
KSTL	1.96	1.96
MHLO	1.98	1.92
NHS1	1.98	1.93

Table 3: The q-values of the coda waves of the 3rd seismic event as Recorded by APE, ARG, KRND, KSTL, MHLO and NHS1 stations of the H.S.N.C.
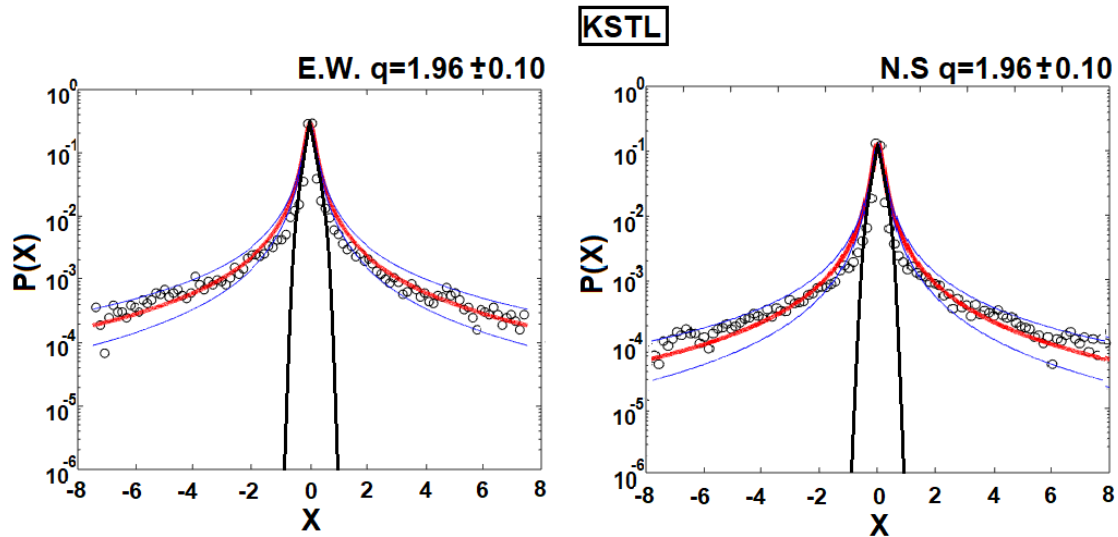
Figure 12: Incremental data of the coda waves from the 3rd event recorded from KSTL station (Black circles) and the fitted Eq 4.2. (Red line).

The 95% Confidence bounds give error $q_{err} = 0.10$ In the East-West component the q-value is q=1.96, same with the North-South component. In the image we also see the Gaussian Curve (Black line) which corresponds to

$$q = 1.$$

The results support the non-extensive character of Seismic coda wave increments as they deviate from the Gaussian behavior and "Heavy tails" are present leading to the conclusion that the seismic coda waves present Long-term memory effects.

Also, the q values are different for each station. This probably links up to their path difference and thus the scatterer differences they encounter through those paths. It is highly probable that the Coda waves indeed carry information linked to the Earth's scatterers.

### 4.1.2. q-Gaussian spectrum in the South Aegean Seismic events

In the literature review of the first chapter we saw that the coda waves exist due to scatterers and the interaction of the latter with the ballistic waves generated by each earthquake event. This occurs due to scattering mechanisms that take place within the earth's crust.

We also saw that the coda waves compose of many different frequencies within the bandwidth of $1 - 50 Hz$ each of which has different characteristics. Also, the attenuation is different for the different frequency bands of the coda waves.

Initiating with this chain of thought we made for the first time a q-spectrum. Meaning that for several frequency bands we found the q-values of the seismogram.

Filter application

We wanted to see the incremental "q" value for each of the $2 - 4\ Hz$, $4 - 8Hz$, $8 - 12\ Hz$ and $12 - 16\ Hz$ frequency bands. The selection of those bands was not random; those were the frequency bands which according to the power spectrum density of the coda waves, hold the highest amount of energy. Also (τι άλλο προσθετω εδώ?) This fact is illustrated in Figures 8,9 Below.
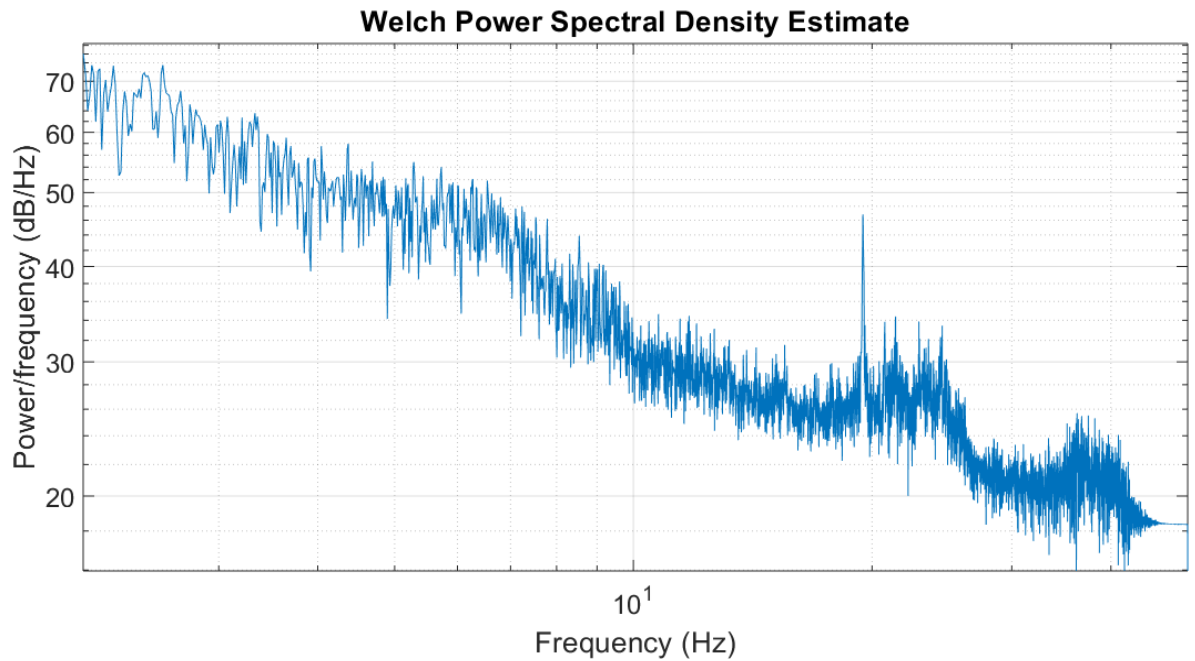
Figure 13: A typical power spectrum density of the First events' Coda waveform
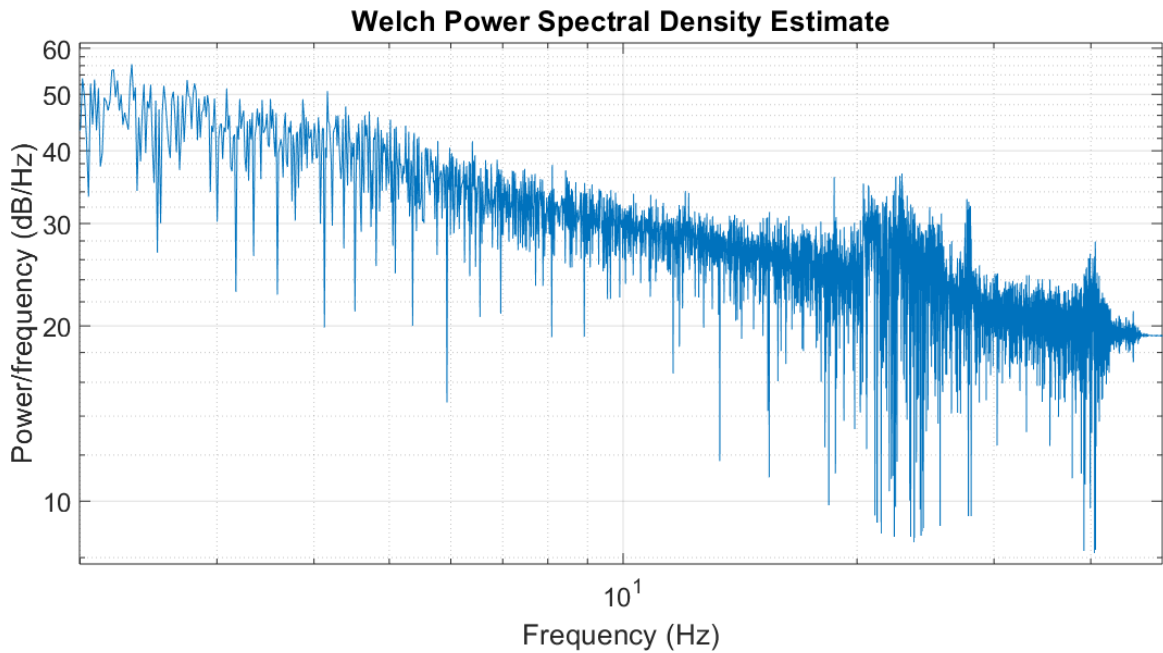
Figure 14: A typical power spectrum density of the second events' Coda waveform.
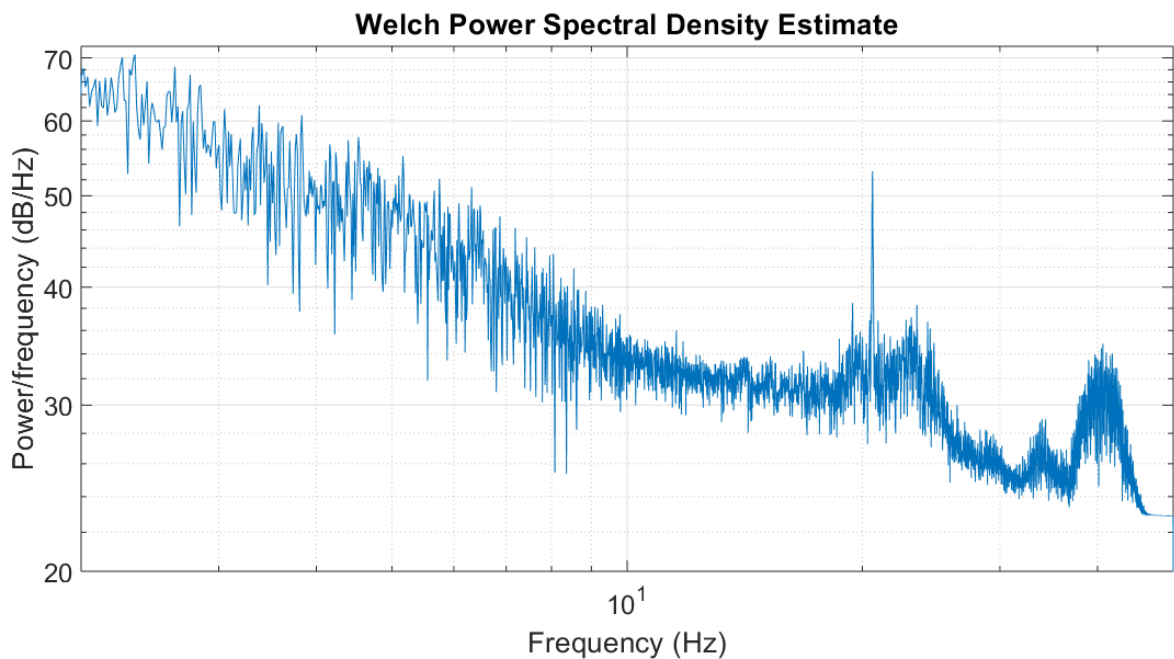
Figure 15: A typical power spectrum density of the Third events' Coda waveform

. In order to have good spectral resolution we used narrow Bandwidth Chebyshev filters of $2-4\ Hz$ width. We then calculated the $q-$value in each window as earlier.

We used Chebyshev filters because we needed a sharp cutoff frequency as the frequency bandwidth of $2-4Hz$ is narrow. Normal Butterworth filters used In the Bibliography don't achieve such a sharp transition because they have flat pass/stop bands. By relaxing the condition of the at pass/stop band we achieve those

sharper cutoffs in our filters [56]. The only drawback is that there is a ripple in the stop band and thus energy leakage. In our case though the ripple is very small and thus the energy leakage does not affect our measurements.

Also because the frequency width of $2Hz$ is very small we weren't able to make a simple band pass filter in matlab so we used a combination of two filters, one low pass and one high pass. For example for the $2 - 4Hz$ filter we made a High pass of $2 - 50\ Hz$ bandwidth as shown in Figure 9 and a low pass of $0 - 4Hz$ bandwidth as shown in Figure 9. In the same manner we constructed all of our filters.
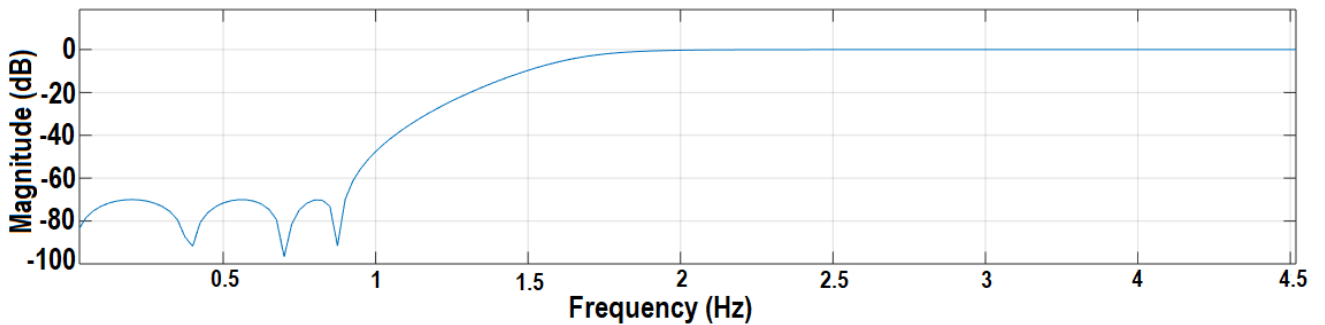

Figure 16: The 2-50 Hz high pass Chebyshev filter. The image is zoomed for better resolution. We are able to see the ripple of the stop-band and the sharp cutoff. The filter needs only ~1 Hz to reach the stop-Band.
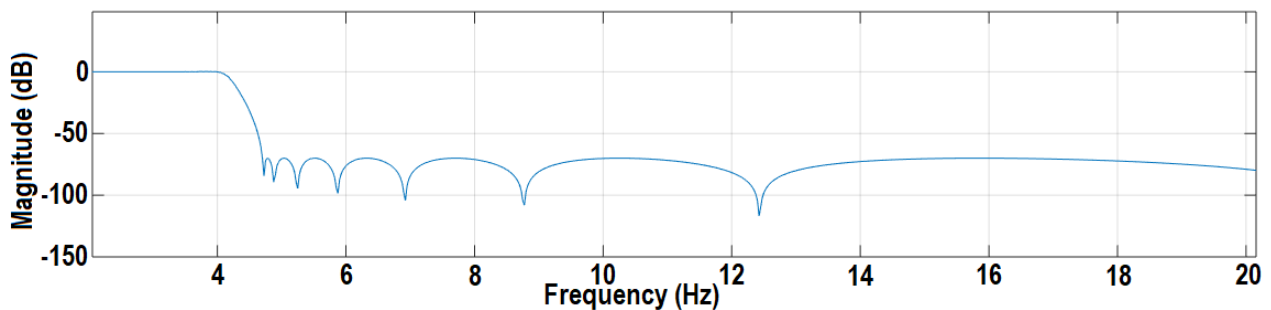

Figure 17: The 0-4 Hz Low pass Chebyshev filter. The image is zoomed for better resolution. we are able to see the ripple of the stop-band and the sharp cutoff. The filter needs only ~1 Hz to reach the stop-Ban

Coda-spectrum N.E.S.P Analysis

After applying the filters and running the analysis of the waveforms presented earlier, the results are given to the tables below:

First event

1st Event	APE	APE	ARG	ARG	KRND	KRND	MHLO	MHLO	NHS1	NHS1

	q_{EW}	q_{NS}	q_{EW}	q_{NS}	q_{EW}	q_{NS}	q_{EW}	q_{NS}	q_{EW}	q_{NS}
Unfiltered	1.85	1.84	1.83	1.82	1.88	1.87	1.98	2.20	1.60	1.59
2-4Hz	2.14	2.09	2.02	2.02	2.12	2.04	2.18	2.18	2.12	2.07
4-8Hz	2.03	2.01	1.97	1.99	1.98	2.05	2.06	2.08	2.01	2.03
8-12Hz	1.98	1.84	1.75	1.75	1.91	1.94	1.94	1.96	1.90	1.87
12-16HZ	1.90	1.78	1.42	1.47	1.85	1.81	1.90	1.94	1.77	1.75

First event East-West q(f) Values

First event North-South q(f) Values
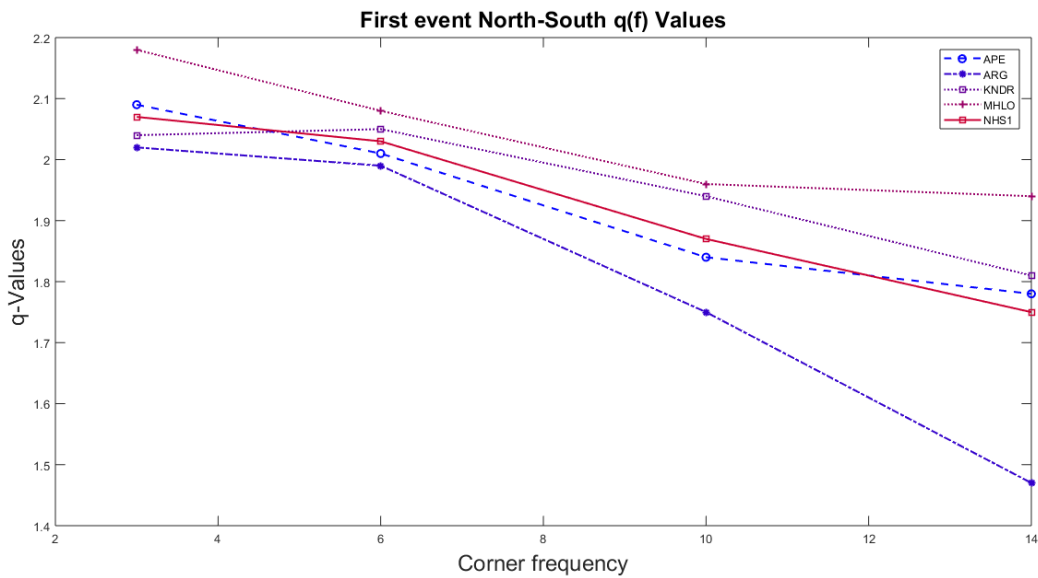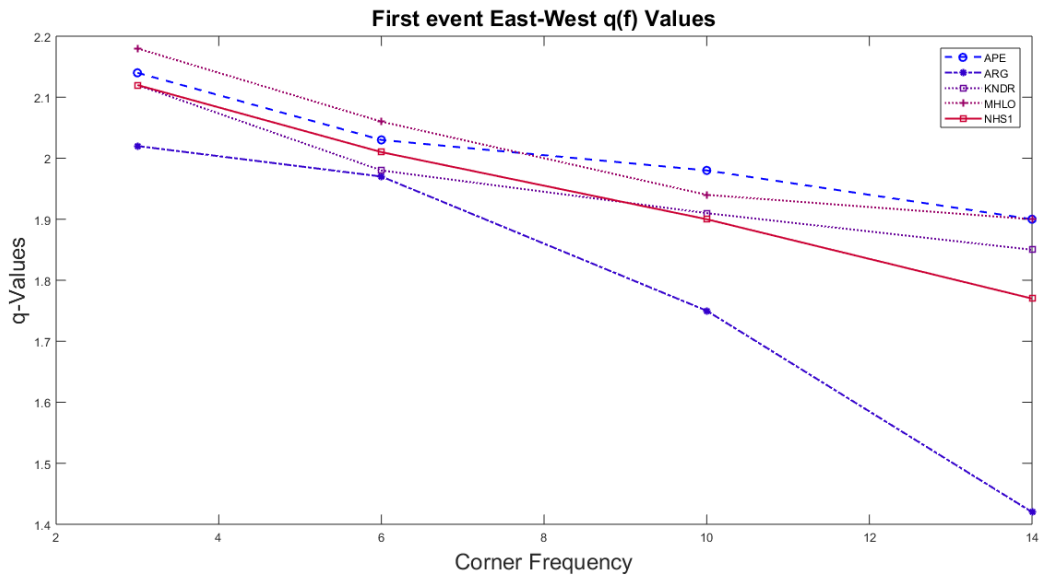
Second Event

2nd Event	ARG	ARG	CHAN	CHAN	KSTL	KSTL	KTHR	KTHR	MHLO	MHLO
	q_{EW}	q_{NS}	q_{EW}	q_{NS}	q_{EW}	q_{NS}	q_{EW}	q_{NS}	q_{EW}	q_{NS}
Unfiltered	1.35	1.37	1.92	1.91	1.92	1.92	1.57	1.58	1.89	1.86

2-4Hz	1.85	1.86	1.99	1.99	2.1	2.1	1.8	1.8	1.9	1.9
4-8Hz	1.65	1.65	1.88	1.89	1.87	1.86	1.58	1.57	1.76	1.6
8-12Hz	1.32	1.43	1.71	1.73	1.78	1.6	1.45	1.4	1.56	1.47

Second event East-West q(f) Values

Second event North-South q(f) Values
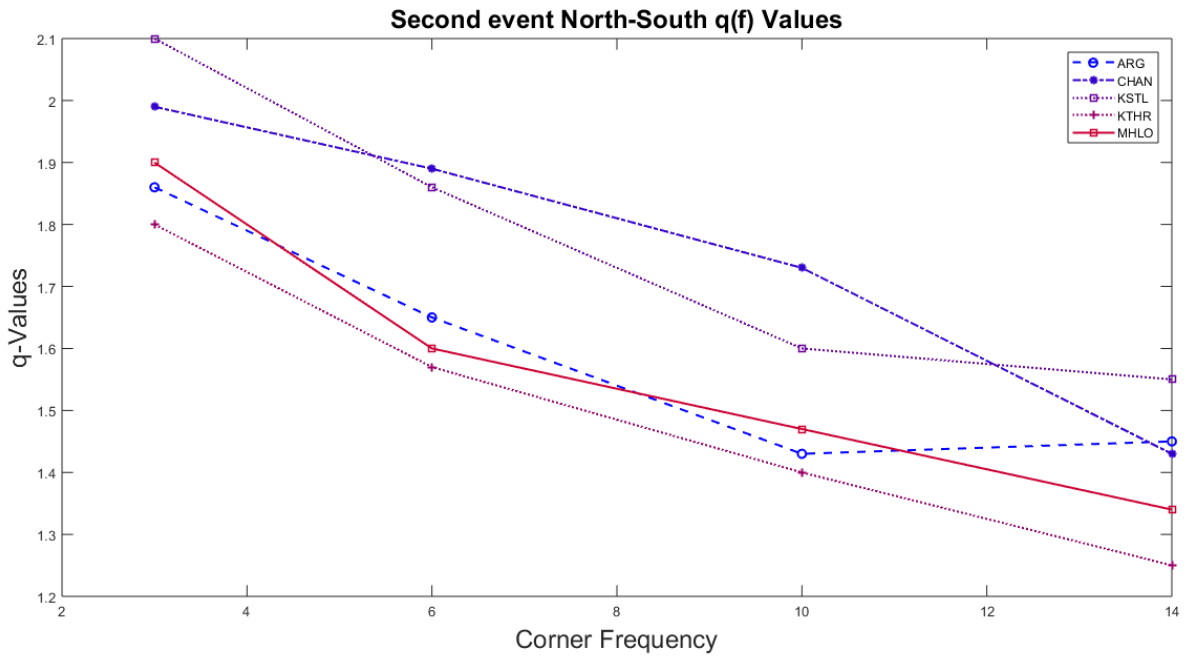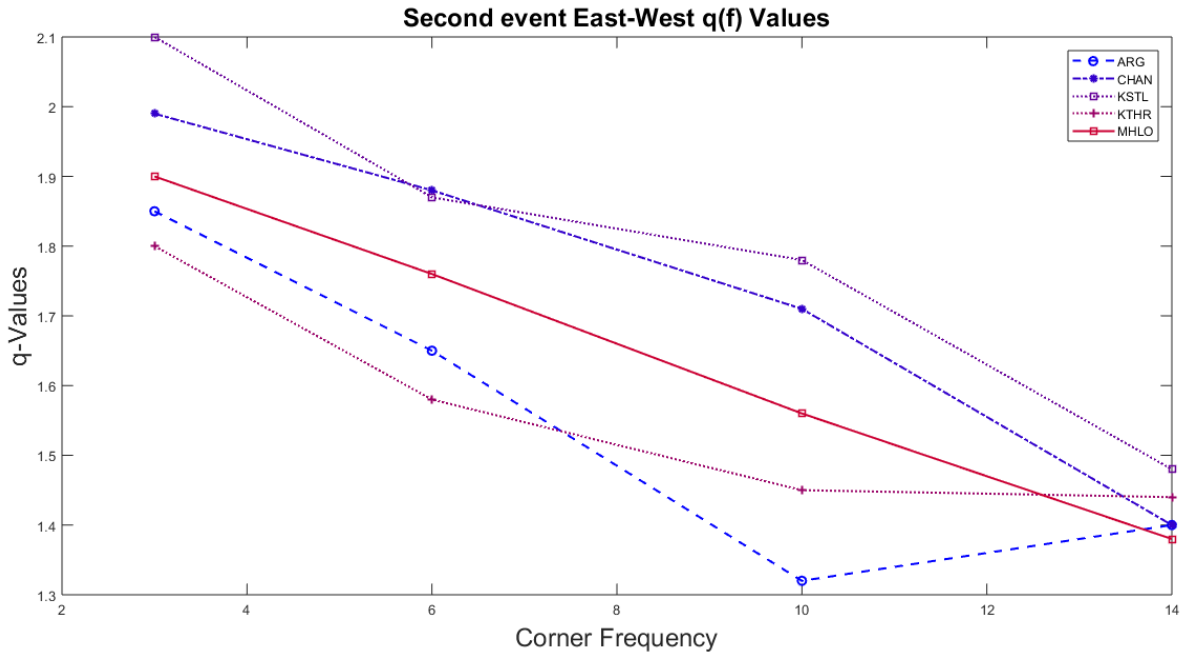
Third Event

3ⁿᵈ Event	APE	APE	ARG	ARG	KRND	KRND	KSTL	KSTL	MHLO	MHLO	NIS1	NIS1
	q_{EW}	q_{NS}	q_{EW}	q_{NS}	q_{EW}	q_{NS}	q_{EW}	q_{NS}	q_{EW}	q_{NS}	q_{EW}	q_{NS}
Unfiltered	1.80	1.80	1.89	1.90	1.83	1.82	2.10	2.10	1.98	1.92	1.98	1.93

2-4Hz	2.15	2.20	2.25	2.20	2.10	2.10	2.10	2.10	2.10	2.10	2.10	2.10
4-8Hz	2.00	1.96	2.05	1.98	1.99	2.00	2.10	2.10	1.93	2.12	1.95	1.94
8-12Hz	1.87	1.84	1.89	2.00	1.70	1.70	1.86	1.81	1.89	1.96	1.64	1.52
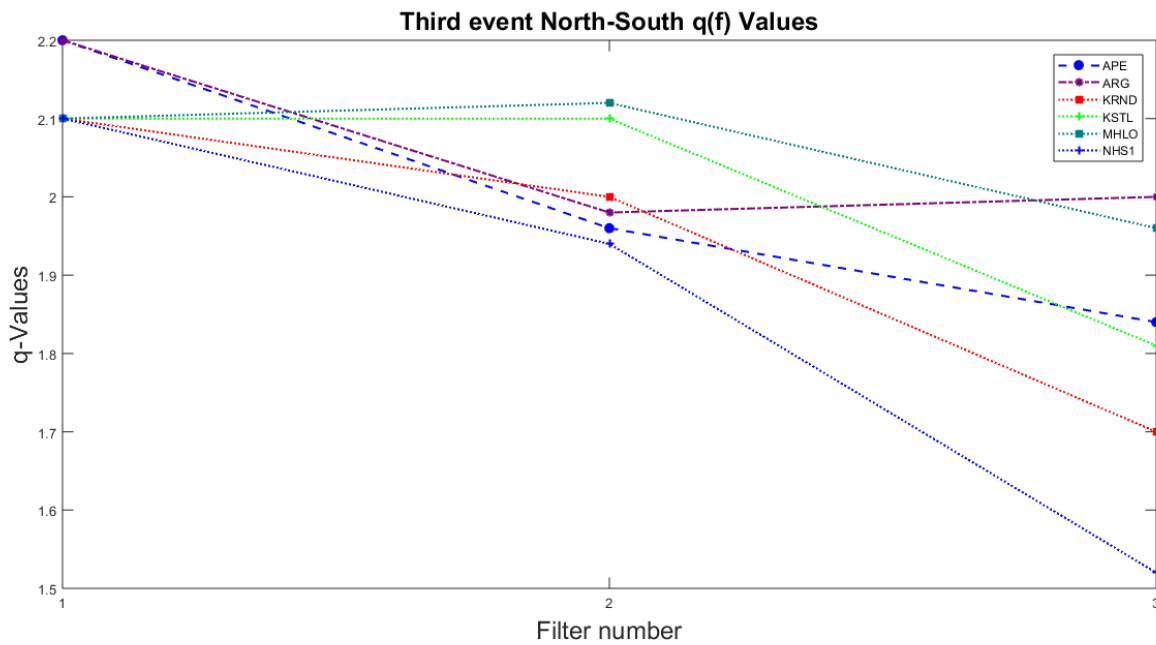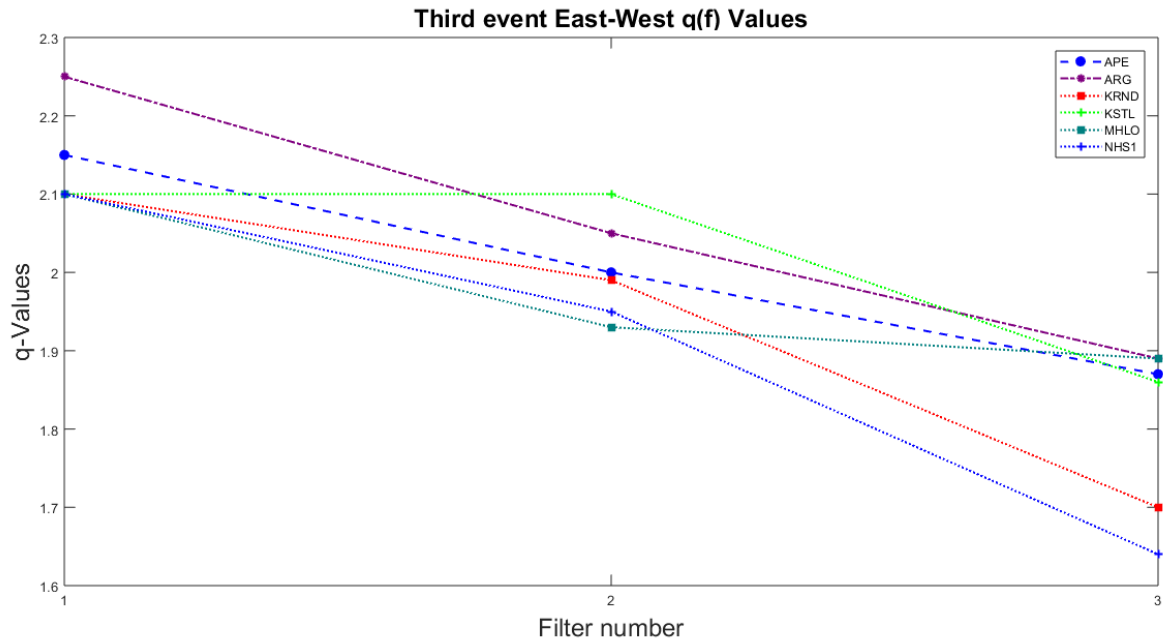
We see that there is an obvious dependence of the q-value to the frequency. And that with increasing frequency, the q value decreases.

4.2.   South Apennines dataset

The next step of our analysis was to study the noise in the second dataset of the INSIEME stations. We are taking advantage of the fact that we have 2 stations with depth difference. One is on ground level and the other in a borehole 50m underground. We will use this fact to check for possible differences of noise and coda wave data with depth.

4.2.1. <u>q-Gaussian noise analysis with depth</u>

In the first part wee studied the dependence of the Non-extensive parameter q with depth. The analysis consists of dividing a daily waveform free of human induced noise into overlapping 30Minute windows with 50% Overlap and running the NESP incremental analysis.

The advantage of the Buried station is that its signal is not corrupted by noise in the same extent with the Ground station. We can easily observe this fact in Figures 15, 16
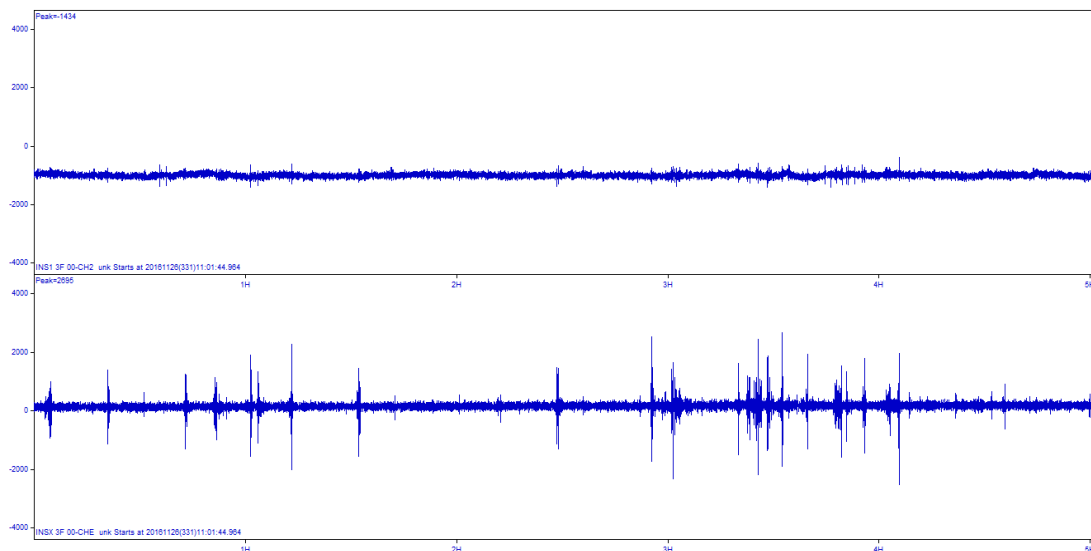

Figure 18: East-West component of the Buried station (above) and the Ground station (Below). The ground station presents persistent spikes and is more corrupted.
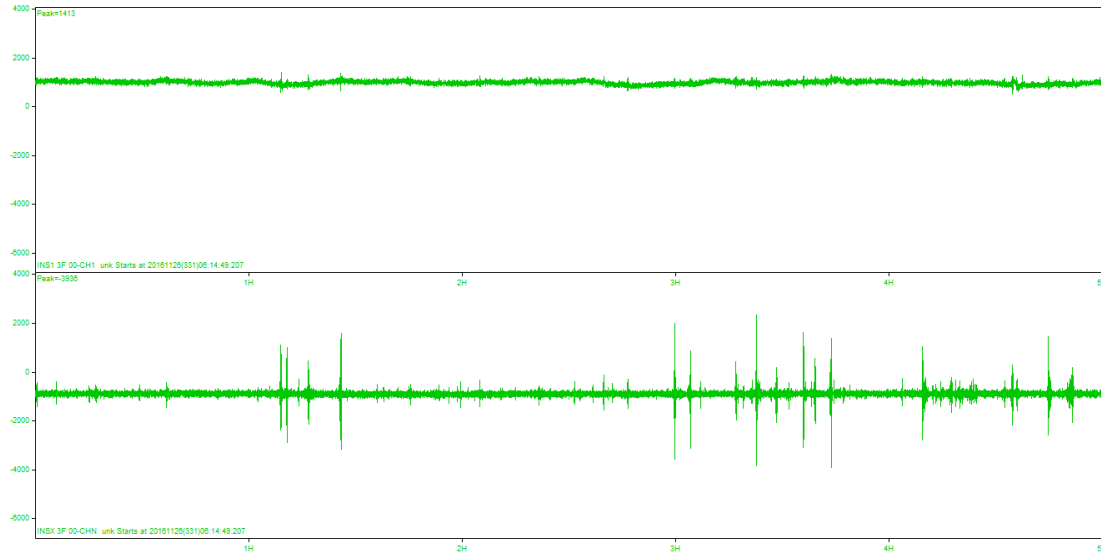
Figure 19: North-South component of the Buried station (above) and the Ground station (Below). The ground station presents persistent spikes and is more corrupted.

We selected 30 Minute windows because on a smilar work conducted [58] it was shown that the q-Value of ambient noise depends on the time window selected and that it was saturated for time windows greater than 20 minutes. So in the 30 minute window the q-value will be saturated. The results are shown in the table and figure below:

Borehole	EW	1.29	1.32	1.30	1.30	1.29	1.29	1.28	1.31	1.31
Borehole	NS	1.42	1.38	1.31	1.21	1.32	1.26	1.25	1.26	1.28
Ground	EW	1.33	1.32	1.39	1.37	1.46	1.62	1.60	1.53	1.51
Ground	NS	1.36	1.59	1.45	1.40	1.40	1.63	1.68	1.60	1.56
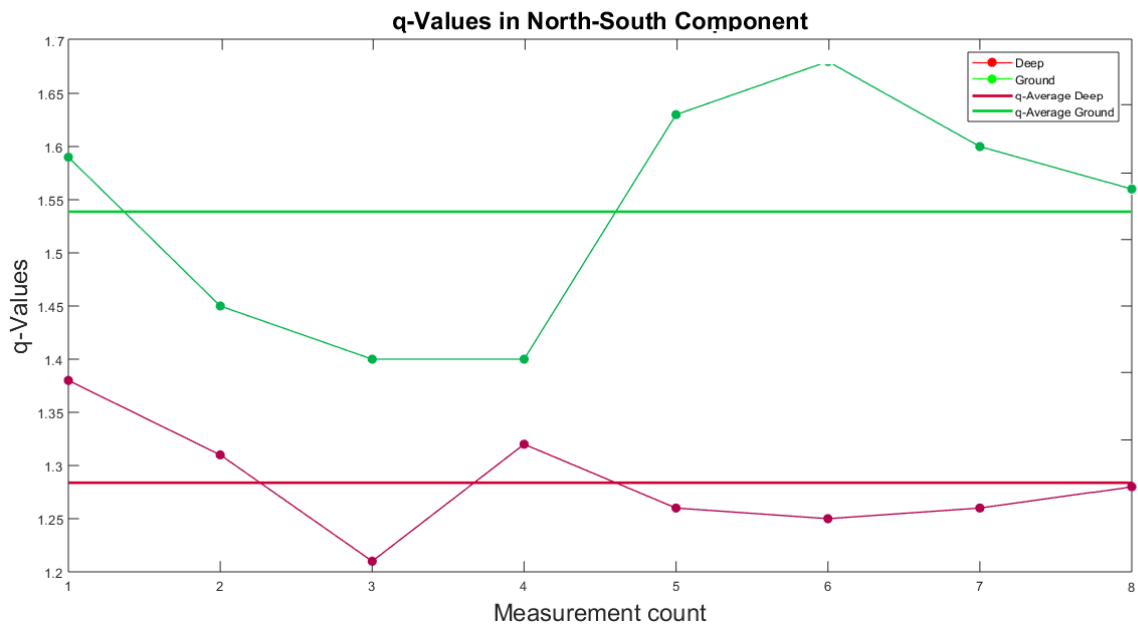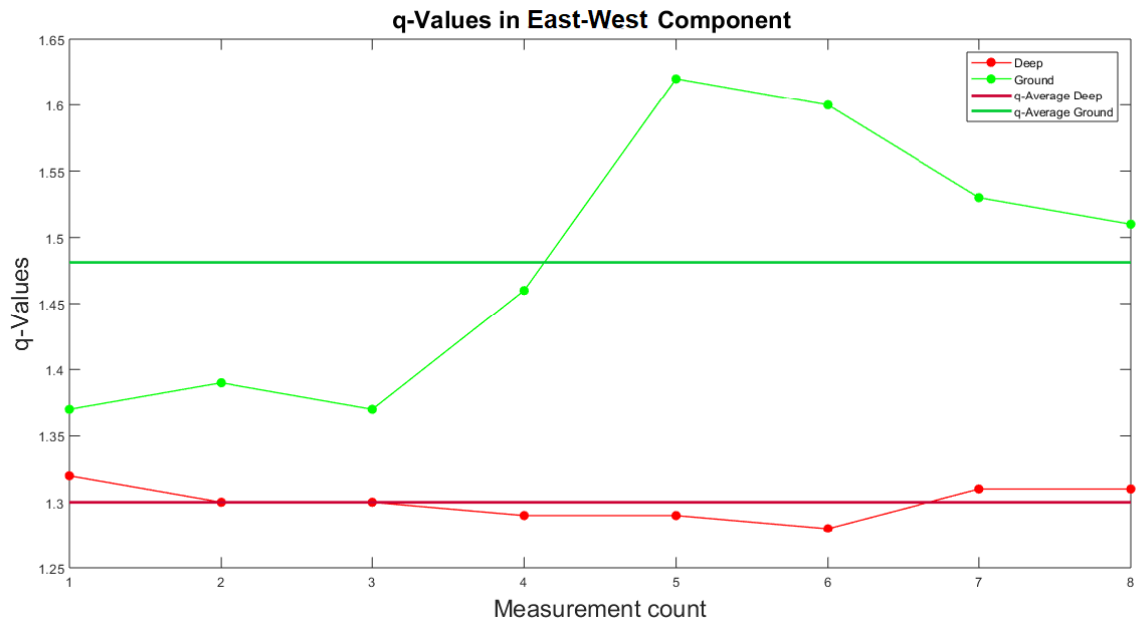
Figure 20: The q-values of the overlapping windows of the Deep (Red colors) and Ground (Green colors) stations in their East-Wens (above) and North-South (below) components. We also see the average q-values of the 2 stations For both components whose values are almost the same. There is a clear difference with depth.
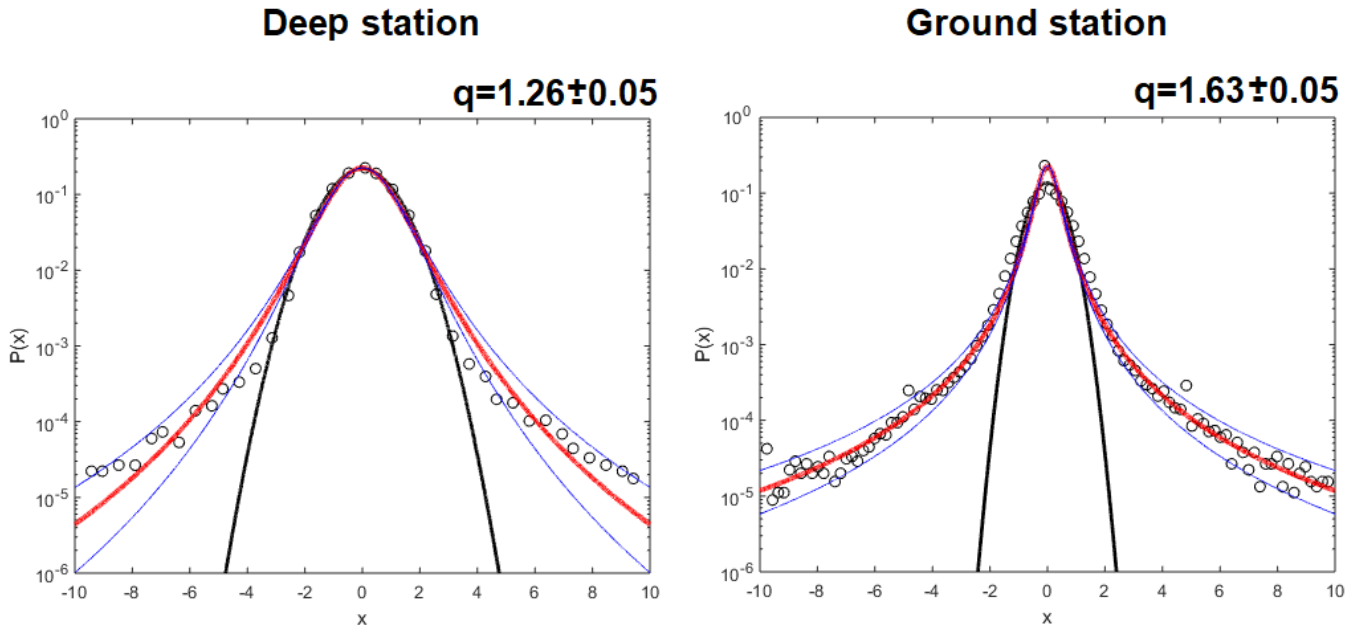
Figure 21: Sample figures of 30 Second Incremental data of the East-West component (seventh measurement in Table above) acquired from the INSIEME stations (Black circles) and fitted to Eq. 4.2 (Red line). The 95% Confidence bounds show error $q_{err} = 0.05$ in both components. The North-South component has the same value as earlier with slight deviation. . In the image we also see the Gaussian Curve (Black line) which corresponds to $q = 1$. There is an obvious bias in the Ground measurement with Higher q-Value probably due to corruption.

We see that there is a difference of the q-Values between the Ground station and the buried station. The q-Average of the Ground station is $q_{Ground}^{EW} = 1.48 \pm 0.10$ For the East-West component and $q_{Ground}^{NS} = 1.54 \pm 0.11$ for the North –South component where The q-Average of the Buried station is $q_{Buried}^{EW} = 1.30 \pm 0.01$ For the East-West component and $q_{Buried}^{NS} = 1.28 \pm 0.05$ for the North –South component. This makes an average of $q_{Ground} \approx 1.47 \pm 0.05$ for the Ground station and $q_{Buried} \approx 1.30 \pm 0.05$ for the buried station.

4.2.2. Coda Wave increment N.E.S.P analysis with depth

The next step in our work was to run the same analysis as in the first part with Coda waves from the two stations of INSIEME and thus seing if the non-extensive parameter-q differs with depth.

The analysis was conducted in the East-west and North-south Components and the results are shown in the table Below:

Event	Borehole station q East-West	Ground station q East-West	Borehole station q North south	Ground station q North south
1	1.73±0.07	1.81±0.06	1.75±0.05	1.79±0.04
2	1.86±0.05	1.86±0.05	1.85±0.07	1.86±0.07
3	1.64±0.06	1.67±0.07	1.69±0.07	1.72±0.07
4	1.77±0.07	1.78±0.07	1.71±0.06	1.75±0.06
5	1.80±0.07	1.67±0.07	1.78±0.06	1.74±0.07

We see that the q-Values remain the same for the Ground as well as the buried stations.

We see a different q-Value for each seismic event, but same q values for each component and depth, both for ground and deep stations. This correlates with a study that found that for single station measurement there was not change of coda wave attenuation with depth between two stations of ground level and in 100m Borehole [18].

5. Discussion

5.1. Coda Increments in the South Aegean

The properties of seismic Coda wave fluctuations are discussed here from the prespective of non-extensive statistical physics. The results support the non-extensive character of seismic coda wave increments as they deviate from the Gaussian behavior and "Heavy tails" are present, leading to the conclusion that coda-waves present long-term memory effects Probably due to the effect of multiscattering caused by the scatterers they encounter in their path.

Those findings are stimulating discussion to further studies that will view seismic wave propagation in complex geostructures in terms of a Tsallis approach.

5.2. Coda q-Value dependence to frequency

In this part and for the first time, we study the frequency dependence of q since the overall q estimated is based on a recording which is the superposition of many harmonic waves. We study the dependence of q in different frequency bands.

A general trend of a decreasing of coda incremental q-Value with frequency is observed for the first time.

5.3. Noise increments q-value difference with depth

In this part we study the incremental q-Values of 30-minute overlapping windows obtained from 2 seismometers, one on the ground and one in a 50m borehole in order to find differences.

The result is that the q-value on the surface is larger. A possible interpretation is that local waves are strongly influenced by local scatterers because noise is composed of local waves "entrapped" within the local

region bounded by scatterers.. The wave field thus represents the local near surface structure and this result is verified by the fact that the values are not the same in the 2 depths.

5.4.   Coda increments in the south Italy

In this part we studied the incremental q-values of coda waves from seismic events in south Italy and northern Greece from the 2 Insieme stations as in the previous part in order to check for depth sensitivity.

The result was that the q-Values in each component were the same on the ground and within the borehole. This verifies the assumption that coda waves' characteristics and content is defined by the scatterers in the far field from the stations and not near field. Our results come in agreement with a previous study that showed that coda attenuation did not change with depth in the same experimental setup with a 100m borehole [18]. Also, comparing our results with that study, we can conclude that the q-Value indeed carries information about the coda-wave attenuation, as both of those characteristics remain unchanged for each seismic event with depth and thus they must carry the same information which is defined by the multiscattering effects within the earth's crust.

Concluding, our work comes in agreement with works that assume the framework of fractal distributed earth to be more suitable [52]. In this way a new path is opened where we can study earth's properties in terms of Tsallis entropy and multifractality as the existence of q in the coda wave increments unveils the bias in the PDFp(x) caused probably due to this "bias".

6. Bibliography

[1] Anache-Ménier D, Van Tiggelen B, Margerin, L. Phase statistics of the seismic coda waves. Phys Rev Lett. 2009 Jun 19;102(24):248501. Epub 2009 Jun 16. DOI: 10.1103/PhysRevLett.102.248501

[2] Keiiti, A. Chouet, B. (1975). Origin of Coda Waves: source, attenuation and scattering effects. Journal of Geophysical Research: Solid Earth. 80. 3322-3342. 10.1029/JB080i023p03322

[3] Chouet, B. (1976). Source, scattering and attenuation effects on high frequency seismic waves. [California data].

[4] Khalturin, T. G., Martynov, V. I., Molnar, V. G., 1978. Preliminary analysis of the spectral content of P and S waves from local earthquakes in the Garm, Tadjikistan region, Bull, seism. Soc. Am., 68: 949–971

[5] Ludovic, M., Bart, T., & Campillo, M., Larose, E., & Sens-Schoenfelder, C & Rossetto, V & Shapiro, Nikolai. (2010). Seismic Coda Waves. 01010. 10.1051/iesc/2010mpcm01010.

[6] Bouchon, M., 1982. The complete synthesis of seismic crustal phases at regional distances, J.Geophys. Res. 87, 1735-1741]

[7] Keiiti, A., 1969. Analysis of the seismic coda of local earthquakes as scattered waves. Journal of Geophysical Research: Solid Earth. 74. Pages 615–631. 10.1029/JB080i023p03322.

[8] Malin, P. E., 1980. A first-order scattering solution for modeling elastic wave codas. I. The acoustic case, Geophys. J. R. Astr. Soc. 63, 361-380.

[9] Levander, A. R., 1985. P-SV resonances in irregular Low-velocity surface layers, Bull. Seism. Soc. Am. 75,847-864

[10] Ru-shan, W., & Keiiti, A. (1988). Introduction: Seismic Wave Scattering in Three-dimensionally Heterogeneous Earth. Pure and Applied Geophysics - PURE APPL GEOPHYS. 128. 1-6. 10.1007/BF01772587.

[11] Matsumoto, S. Characteristics of Coda Waves and Inhomogeneity of the Earth, Journal of Physics of the Earth, 1995, Volume 43, Issue 3, Pages 279-299, Released April 30, 2009, Online ISSN 1884-2305, Print ISSN 0022-3743, https://doi.org/10.4294/jpe1952.43.279

[12] Haruo, S. (1984). Attenuation and envelope formation of three-component seismograms of small local earthquakes in randomly inhomogeneous lithosphere. Journal of Geophysical Research. 89. 1221-1241. 10.1029/JB089iB02p01221

[13] Carcolé, E. and Sato, H. (2010), Spatial distribution of scattering loss and intrinsic absorption of short-period S waves in the lithosphere of Japan on the basis of the Multiple Lapse Time Window Analysis of Hi-net data. Geophysical Journal International, 180: 268-290. doi:10.1111/j.1365-246X.2009.04394.x

[14] Hedlin, M.A. & Shearer, P.M., 2002. Probing mid-mantle heterogeneity using PKP Coda waves, Phys. Earth planet inter., 130, 195-208.

[15] Aki, K., Tsujiura, M., Hori, M. and Goto, K., 1958. Spectral study of near earthquake waves. Bull. Earthquake Res. Inst., Univ. Tokyo, 36: 71-98.

[16] Aki, K., Tsujiura, M., 1959. Corellation study of near earthquake waves. Bull. Earthquake Res. Inst., Univ. Tokyo 37: 203-232.

[17] Spudich, P., Bostwick, T. Studies of the seismic coda using an earthquake cluster as a deeply buried seismograph array. Journal of Geophysical Research: Solid Earth 92 (B10), 10526-10546].

[18] Aki, K. (1980), Scattering and attenuation of shear waves in the lithosphere, *J. Geophys. Res.*, 85(B11), 6496–6504, doi: 10.1029/JB085iB11p06496.

[19] Sato, H. Study of seismogram envelopes based on scattering by random inhomogeneities in the lithosphere: a review. Physics of the Earth and Planetary Interiors. Volume 67, Issues 1–2. 1991, pages 4-19. ISSN 0031-9201. https://doi.org/10.1016/0031-9201(91)90056-N.

[20] Bettina, G,A., Shearer, P,M., Egill, H. (2008). Spectral Discrimination between Quarry Blasts and Earthquakes in Southern California. Bulletin of the Seismological Society of America. 98. 10.1785/0120070215.

[21] Trégourès, N., Hennino, R., Lacombe, C., Shapiro, N., M., Margerin, L., Campillo, M., Van Tiggelen, B., A., Multiple scattering of seismic waves. Ultrasonics, Volume 40, Issues 1–8, 2002, Pages 269-274, https://doi.org/10.1016/S0041-624X(02)00105-1.

[22] Dainty, A.M., and Toksoz, M.N., 1981. Seismic codas on the earth and the moon: A comparison. Phys. Earth Planet. Inter., 26:250-260.

[23] Wesley, J.P., 1965. Diffusion of seismic energy in the near range. J. Geophys. Res., 70: 5099-5106.

[24] Jwngsar, B. (2012). Estimation of Coda Wave Attenuation Quality Factor from Digital Seismogram Using Statistical Approach. SCIENCE AND TECHNOLOGY. 2. 1-7. 10.5923/j.scit.20120201.01.

[25] Morozov I. B. Zhang. C. Duenow. J. N. Morozova E. A. Smithson. S. B., 2008. Frequency dependence of coda Q: Part I. Numerical modeling and examples from Peaceful Nuclear Explosions. Published in: Bull. Seism. Soc. Am., 98, 2008, pp. 2615–2628, doi: 10.1785/0120080037.

[26] Morozov I. B., 2008. Geometrical attenuation, frequency dependence of Q, and the absorption band problem. Geophysical Journal International, Volume 175, Issue 1, 1 October 2008, Pages 239 252,doi:10.1111/j.1365-246X.2008.03888.x

[27] Morozov. I., B. Temporal variations of coda Q: An attenuation-coefficient view. Physics of the Earth and

Planetary Interiors, Volume 187, Issues 1–2. 2011. Pages 47-55, https://doi.org/10.1016/j.pepi.2011.04.012.

[28] Obermann, A.., Planès T., Larose, E., Sens-Schönfelder, C., Campillo, M. Depth sensitivity of seismic coda waves to velocity perturbations in an elastic heterogeneous medium, Geophysical Journal International, Volume 194, Issue 1, 1 July 2013, Pages 372 382, https://doi.org/10.1093/gji/ggt043

[29] Takemura, S., Furumura, T., Maeda, T., Scattering of high-frequency seismic waves caused by irregular surface topography and small-scale velocity inhomogeneity, Geophysical Journal International, Volume 201, Issue 1, 1 April 2015, Pages 459–474, https://doi.org/10.1093/gji/ggv038

[30] A., Wennerberg, L,. Energy-flux model of seismic coda: Separation of scattering and intrinsic attenuation. Bulletin of the Seismological Society of America. 1987. 77 (4): 1223–1251. 2-4 5-10 10-20 25-35 Hz

[31] Kikuchi, M., 1981. Dispersion and attenuation of elastic waves due to multiple scattering from inclusions, Physics of the Earth and Planetary Interiors, volume 25, issue 2, pages 159-162,

[32] Sykes, L. R., and J. Oliver, The propagation of short-period seismic surface waves across oceanic area, Bull. Seismol. $oc. Am., 54, 1349-1416, 1964.

[33] Kizawa, T., and R. Yamaguti, Some new phases observed in a study of earthquake swarms relating to volcanic activity, 2, Geophys. Mag., 30, 93-129, 1960.

[34] Scherbaum, F. and Sato, H., (1991). Inversion of full seismogram envelopes based on the parabolic approximation: Estimation of randomness and attenuation in southeast Honshu, Japan. J. Geophys. Res., in press. 10.1029/90JB01538.

[35] Sato H. (1984).Scattering and attenuation of seismic waves in the lithosphere: single scattering theory in a randomly inhomogeneous medium (in japaneese). Rep. Nat. Res. Ctr. Disaster. Prevention. 33: 101-186

[36] Sato H. (1990). Unified approach to amplitude attenuation and coda extension in the randomly inhomogeneous lithosphere. Pure and Applied Geophysics PAGEOPH. 132. 93-121. 10.1007/BF00874359.

[37] Sato H. (1988a) Is the Single Scattering Model Invalid for the Coda Excitation at Long Lapse Time?. In: Aki K., Wu RS. (eds) Scattering and Attenuations of Seismic Waves, Part I. Pageoph Topical Volumes. Birkhäuser, Basel.

[38] Kopnichev, Y.F., A model of generation of the tail of the seismogram. Dokl. Akad. SSSR, 222: 333-335 (in Russian)

[39] Gao, L.S., Biswas, N.N., Lee, L.C, and Aki, K., 1983a. Effects of multiple scattering on coda waves in three dimentional space. Pure Appl. Geophys., 121: 3-15.

[40] Gao, L.S., Lee, L.C, Biswas, N.N., and Aki, K., 1983b Comparison of the effects between single and multiple scattering on coda waves for local earthquakes. Bull. Seismol. Soc. Am., 73: 377-389.

[41] Gusev, A.A. and Abubakiov, I.R., 1987. Monte-Carlo simulation of record envelope of a near earthquake. Phys. Earth Planet. Inter., 49:30-36.

[42] Hoshiba,M., 1991. Simulation of multiple scattered coda wave excitation based on the energy conservation Law. Phys. Earth Planet. Inter., 67: 123-136.

[43] Obara, K. and Sato, H., 1988. Numerical simulation of coda envelopes including reflection phase (in Japaneese). Prog. Abst. Seismol. Soc. Japan, 2:B 76

[44] Hans E, H. Hartse, W. Scott Phillips, Michael C. Fehler, Leigh S. House; Single-station spectral discrimination using coda waves. Bulletin of the Seismological Society of America. 1995. 85 (5): 1464–1474.

[45] Kawahara., J. and Yamashita., T. Scattering of elastic waves by a fracture zone containing randomly distributed cracks. 1992. pure and applied geophysics vol 139 is 1 pp 121-144.

[46] Flatté, S. M., and R.-S. Wu (1988), Small-scale structure in the lithosphere and asthenosphere deduced from arrival time and amplitude fluctuations at NORSAR, J. Geophys. Res., 93(B6), 6601–6614, doi:10.1029/JB093iB06p06601.

[47] Line, C.E.R., Hobbs, R.W., Hudson, J.A. &Synder, D.B., 1998. Statistical inversion of controlled-source seismic data using parabolic wave scattering theory, Geophys. J. Int., 132., 61-78.

[48] Jin, A., T. Cao, and K. Aki, Regional change of coda Q in the oceanic lithosphere, J. Geophys. Res., 90, 8651-8659,1985.

[49] Jin, A., and K. Aki, Temporal change in coda Q before the Tangshan earthquake of 1976 and the Haicheng earthquake of 1975, J. Geophys. Res., 91, 665-673, 1986.

[50] Anton M. Dainty, Robert M. Duckworth, An Tie; Attenuation and backscattering from local coda. Bulletin of the Seismological Society of America (1987); 77 (5): 1728–1747.

[51] Nishigami K., 1991. A new inversion method of Coda waveforms to determine spatial distribution of Coda scatterers in the crust and uppermost mantle. Geophys. Res. Lett. Vol. 18 Is. 12 P. 2225-2228.

[52] Alexander A. Gusev, Iskander R. Abubakirov; Simulated envelopes of non-isotropically scattered body waves as compared to observed ones: another manifestation of fractal heterogeneity, Geophysical Journal International, Volume 127, Issue 1, 1 October 1996, Pages 49–60, https://doi.org/10.1111/j.1365-246X.1996.tb01534.x.

[53] Tsallis, C., (2009). Introduction to nonextensive statistical mechanics: Approaching a complex world. 10.1007/978-0-387-85359-8.

[54] Gibbs J. W. Elementary principles in statistical mechanics. page 14, 1902.

[55] Hloupis, G., Papadopoulos, I., Makris, J. P., Vallianatos, F. (2013). The south Aegean seismological network –HSNC. Advances in Geosciences, 34, 15-21

[56] A. L. Ronald and D. W. Mills. Signal Analysis Time, Frequency, Scale and Structure. 2004.

[57] Koutalonis, Ioannis & Vallianatos, Filippos. (2017). Evidence of Non-extensivity in Earth's Ambient Noise. Pure and Applied Geophysics. 174. 10.1007/s00024-017-1669-9.

[58] T. G. Rautian, V. I. Khalturin; The use of the coda for determination of the earthquake source spectrum. *Bulletin of the Seismological Society of America* ; 68 (4): 923–948.

[59] Vallianatos, F., Benson, P., Meredith, P., & Sammonds, P. (2012). Experimental evidence of a non-extensive statistical physics behavior of fracture in triaxially deformed Etna basalt using acoustic emissions. Europhysics Letters, 97(58002), 2012.

[60] Papadakis, G., Vallianatos, F., & Sammonds, P. (2014). A nonextensive statistical physics analysis of the 1995 Kobe, Japan earthquake. Pure and Applied Geophysics, 172, 1923–1931.

[61] Burlaga, L. F., & Vinas, A. F. (2005). Tsallis distribution of the largescalemagnetic field strength fluctuations in the solar wind from 7 to 87 AU. Journal of Geophysical Research, 110, A07110.

[62] Tony Alfredo Stabile and the INSIEME Team (2016): SIR-MIUR Project INSIEME - broadband seismic network in Val d'Agri (souther Italy). International Federation of Digital Seismograph Networks. Other/Seismic Network. 10.7914/SN/3F_2016

[63] Andronikidis, N., Kokinou, E., Vafidis, A. et al. Mar Geophys Res (2018) 39: 475. https://doi.org/10.1007/s11001-017-9337-0

[64] Higgins, Michael. (2009). Geology of the Greek Islands.

[65] Patacca, Etta & Scandone, Paolo. (2007). Geology of the Southern Apennines. Bollettino - Societa Geologica Italiana. 7. 75-112.

[66] KNOTT S.D. (1987) - The Liguride complex of southern Italy - a Cretaceous to Paleogene accretionary wedge. Tectonophysics, 142, 217-226.

[67] KNOTT S.D. (1994) - Structure, kinematics and metamorphism in the Liguride Complex, southern Apennines, Italy. Journ. Struct. Geol., 16 (8), 1107-1120

[68] MILLI S. & MOSCATELLI M. (2000) - Facies analysis and physical stratigraphy of the Messinian turbiditic complex in the Valle del Salto and Val di Varri (Central Apennines). G. Geol., 62, 57-77